






Restoring tendon microenvironment in tendinopathy: Macrophage modulation and tendon regeneration with injectable tendon hydrogel and tendon-derived stem cells exosomes

Danmei Li^{a,1}, Shuai Li^{a,1} , Shukun He^{a,1}, Hongpu He^a, Guangxun Yuan^a , Binbin Ma^a, Yijun Zhang^a, Chengjie Yuan^a, Zhiqin Liu^b, Zhenhan Deng^{c,d,**} , Jian Xu^{a,*}

^a Department of Orthopedics, The First Affiliated Hospital, Zhejiang University School of Medicine, Hangzhou, 310003, China

^b Department of Orthopaedics, Zhuzhou Hospital Affiliated to Xiangya School of Medicine, Central South University, 412007, China

^c Department of Orthopaedics, The First Affiliated Hospital of Wenzhou Medical University, Wenzhou, Zhejiang, 325000, China

^d Geriatrics Center, The First Affiliated Hospital of Wenzhou Medical University, Wenzhou, 325000, Zhejiang, China

ARTICLE INFO

Keywords:

Tendinopathy
Macrophage
Tendon-derived stem cell exosomes
Tendon-derived extracellular matrix
Hydrogel

ABSTRACT

Tendinopathy is a common musculoskeletal disorder in which a significant number of patients do not attain effective therapeutic outcomes. The extent of the inflammatory response and the dynamics of collagen synthesis metabolism are critical factors that influence the intrinsic self-repair capacity of tendons. However, the poor microenvironment within the tendon significantly impedes the self-repair process in tendinopathy. In this study, an injectable tendon-derived decellularized extracellular matrix (tdECM) hydrogel was utilized to treat tendinopathy. This hydrogel provides a more cytocompatible microenvironment while retaining certain bioactive factors of native tendon extracellular matrix (ECM), compared to collagen hydrogel. Notably, it was discovered for the first time that the tdECM hydrogel promotes M2 macrophage polarization, thereby exerting an anti-inflammatory effect in vivo. Furthermore, utilizing tdECM as a carrier for the sustained release of tendon-derived stem cells exosomes (TDSCs-Exos), our findings from both in vitro and in vivo studies indicate that the tdECM hydrogel, in conjunction with exosomes, demonstrated a pronounced synergistic enhancement in modulating inflammation, promoting M2 macrophage polarization, and facilitating tendon regeneration and repair efficacy. These results suggest its potential as a promising therapeutic strategy for tendon disorders.

1. Introduction

Tendinopathy is a prevalent musculoskeletal disorder, primarily presenting with chronic pain and diminished function, particularly among athletes and the elderly [1]. This condition is characterized by inflammation and degenerative changes in the tendon, which can ultimately result in tendon tears and ruptures [2]. The prevalence of Achilles tendon disease is 5.9% in the general population, increasing to 13.7–23.9% in athletes [3,4]. In athletes, tendinopathy can lead to a substantial decline in training, competition, and overall athletic performance, potentially culminating in the premature termination of their

athletic careers. For the general population, this type of disease can impair joint function, subsequently diminishing the quality of daily life and work, and potentially resulting in joint disability. Patients frequently necessitate recurrent medical consultations, thereby imposing significant social and economic burdens. Despite the availability of various contemporary treatments, a significant proportion of patients continue to experience unresolved tendon symptomatology. This therapeutic ineffectiveness may be attributed to the adverse microenvironment, which influences both the magnitude of the inflammatory response and the dynamics of collagen synthesis metabolism—two critical factors that significantly affect the intrinsic self-repair

* Corresponding author. Department of Orthopedics, The First Affiliated Hospital, Zhejiang University School of Medicine, Hangzhou, 310003, China.

** Corresponding author. Department of Orthopaedics, The First Affiliated Hospital of Wenzhou Medical University, Wenzhou, Zhejiang, 325000, China.

E-mail addresses: lmd122@126.com (D. Li), allenle1991@sina.com (S. Li), dkdkdkhsk@163.com (S. He), 22318631@zju.edu.cn (H. He), 12418671@zju.edu.cn (G. Yuan), binbin.ma@zju.edu.cn (B. Ma), zhangyijun87@zju.edu.cn (Y. Zhang), yuancjors@zju.edu.cn (C. Yuan), zhiqin_liu@csu.edu.cn (Z. Liu), dengzhenhan@wmu.edu.cn (Z. Deng), 0022029@zju.edu.cn (J. Xu).

¹ These authors contributed equally to this work.

<https://doi.org/10.1016/j.bioactmat.2025.01.016>

Received 12 October 2024; Received in revised form 23 December 2024; Accepted 14 January 2025

2452-199X/© 2025 The Authors. Publishing services by Elsevier B.V. on behalf of KeAi Communications Co. Ltd. This is an open access article under the CC BY-NC-ND license (<http://creativecommons.org/licenses/by-nc-nd/4.0/>).

capacity of tendons [5,6].

Macrophages are increasingly recognized as pivotal contributors to tissue homeostasis, tendon development, and repair through their dual role in promoting tissue repair and mitigating inflammation [6–8]. Consequently, ameliorating the microenvironment of diseased tendons to facilitate collagen synthesis, alongside the modulation of macrophages, is crucial for the effective repair of tendinopathy. Furthermore, several studies have indicated that the dysregulation of the extracellular matrix (ECM) is also associated with the pathogenesis of tendinopathy [2,9]. Tendon-derived decellularized extracellular matrix (tdECM) hydrogel comprises extracellular matrix products obtained from natural tendons following a decellularization protocol that ensures low immunogenicity [10,11]. The hydrogel offers additional bioactive components compared to conventional collagen hydrogels, thereby enhancing the microenvironment conducive to tissue remodeling [12–14].

Decellularized extracellular matrix (dECM) hydrogels derived from diverse sources have been extensively utilized in the fields of cardiology, cartilage repair, and neurology, among others. Notably, most of these hydrogels have been administered in injectable form [15,16]. As an innovative injectable scaffold for tissue engineering, tdECM hydrogel has shown the potential in facilitating tendon repair [12]. However, the current research on injectable tdECM hydrogel is still mainly focused on its role in promoting collagen synthesis in vitro [12,17]. In recent years, ECM has been suggested to influence macrophage polarization [18–20]. ECM derived from small intestinal submucosa has been demonstrated to promote the polarization of M2 macrophages, thereby facilitating the treatment of ulcerative colitis [18]. Nonetheless, the application of natural ECM for the regulation of macrophage polarization in the context of tendinopathy remains limited [21].

Exosomes (Exo), which are cellular vesicles with diameters ranging from 50 to 200 nm, transport biologically active RNA or DNA [22]. They enable intercellular communication by binding to specific receptors on the surface of target cells [23]. Recent studies have identified that one of the fundamental mechanisms by which exosomes contribute to tissue

healing is through their immunomodulatory effects. Specifically, exosomes derived from stem cells exhibit significant potential in regulating macrophage polarization [24–26]. Tendon-derived stem cells exosomes (TDSCs-Exos) have been reported to facilitate the healing of ruptured tendons and tendinopathy by modulating macrophage polarization [27, 28]. However, the precise anti-inflammatory mechanisms underlying these effects remain unclear. Free exosomes face challenges in remaining localized at the site of tendon injury, often dispersing or being rapidly cleared. Consequently, there is a need for an exosome delivery system to ensure sustained release for effective tendinopathy repair. Injectable hydrogels, particularly those enriched with collagen and growth factors, such as tdECM, are anticipated to enhance anti-inflammatory and pro-tendon repair outcomes when employed as exosome carriers.

The tdECM hydrogel, which was enriched with collagen and growth factors, was utilized in this study to optimize the intrinsic self-repair capacity of tendons and to realize the long-term role of exosomes in tendons. This method facilitates the repair of tendinopathy by enhancing the tendon microenvironment and achieving the sustained release of exosomes. The primary objective is to investigate the impact and correlation between the tdECM hydrogel and TDSCs-Exos on M2 polarization and tendon repair both in vitro and in vivo. In this study, we initially investigated the properties of tdECM hydrogel and assessed the impact of varying concentrations of TDSCs-Exos on tendon differentiation and anti-inflammatory responses. Subsequently, we evaluated the sustained-release efficiency of TDSCs-Exos within the tdECM hydrogel. We then examined the combined effects of tdECM hydrogel and TDSCs-Exos both in vivo and in vitro, focusing on tendon differentiation and macrophage polarization. Our hypothesis posits that the integration of tdECM hydrogel with TDSCs-Exos exerts a synergistic effect on tendinopathy healing by enhancing tendon differentiation and modulating macrophage polarization (Fig. 1).

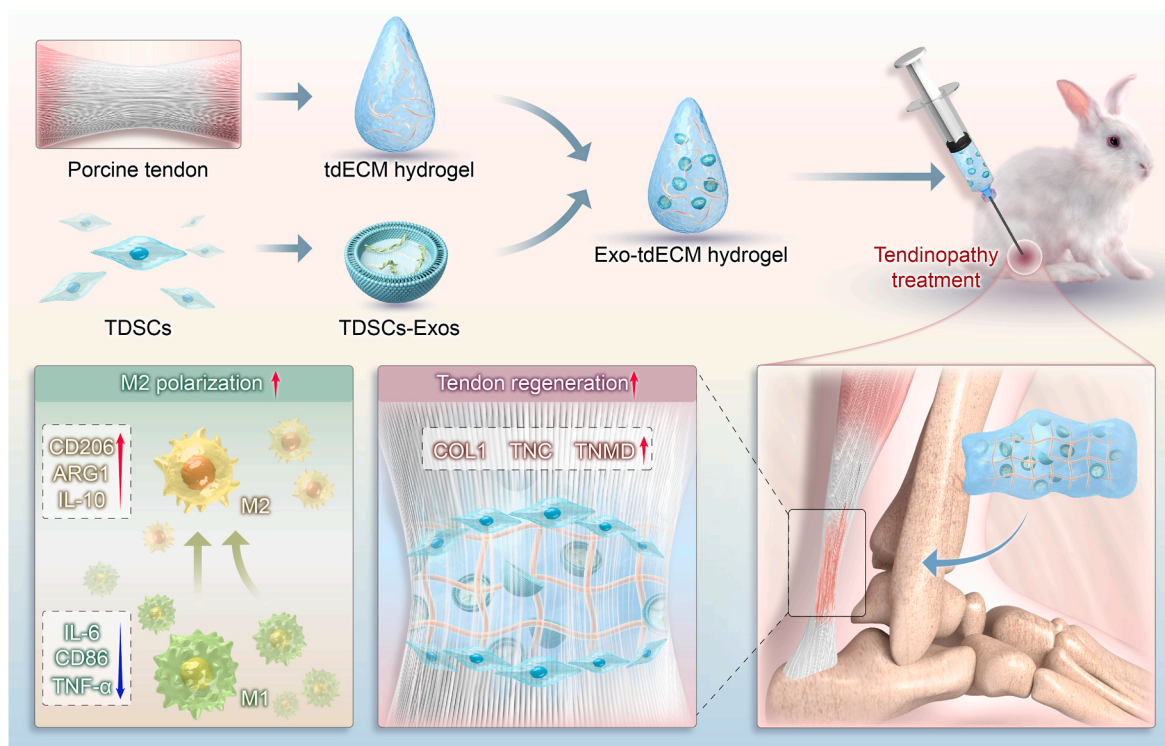


Fig. 1. Schematic diagram of the application of tdECM hydrogel loaded with tendon-derived stem cells exosomes (TDSCs-Exos) in ameliorating the microenvironment associated with tendinopathy. This treatment enhances M2 macrophage polarization and promotes the differentiation of tendon-derived stem cells (TDSCs) alongside the synthesis of type I collagen, thereby facilitating the repair process in tendinopathy. Exo-tDECm hydrogel: tdECM hydrogel with TDSCs-Exos.

2. Methods

2.1. Decellularization of tendon

Porcine Achilles tendon tissues were obtained from a local butcher and subsequently washed with distilled water (DiH₂O) for 24 h. Following the washing step, the tissues were incubated in a 0.05 % Trypsin-EDTA solution (Solarbio, Beijing, China) for 1 h. The Trypsin-EDTA solution was then replaced with a 2 % Triton-X 100 (v/v) solution (Solarbio, Beijing, China) and 1.5 % Peracetic Acid (PAA) (Sypot, Fujian, China) for 4 h. This was followed by two washes in DiH₂O, each lasting 3 h at 37 °C. The samples were then treated with a 5 % Sodium bicarbonate (NaHCO₃) solution (Aladdin, Shanghai, China) for 8 h and thoroughly washed in DiH₂O for one week, with the solution being exchanged daily. Finally, the samples were frozen at –80 °C.

2.2. Characterizations of tdECM

The effectiveness of decellularization was evaluated through Deoxyribonucleic Acid (DNA) quantification assays, hematoxylin and eosin (H&E) staining, and 4',6-diamidino-2-phenylindole (DAPI) staining. Additionally, the collagen components in the decellularized tissue were assessed. The dsDNA content of both native and decellularized tissues was extracted using the Universal Genomic DNA Purification Mini Spin Kit (Beyotime, Shanghai, China) and quantified with a spectrophotometer (Thermo Scientific Nano-Drop, USA). The collagen content was determined by measuring the amount of hydroxyproline (HYP) using the Hydroxyproline Content Assay Kit (Solarbio, Beijing, China) and a spectrophotometer (Thermo Scientific Nano-Drop, USA).

The ultrastructure of the decellularized tendon tissues was examined using scanning electron microscopy (SEM) (FEI Quanta250, USA). The samples were fixed at 4 °C using 2.5 % glutaraldehyde for 12 h. Subsequently, the samples were rinsed with 0.1M phosphate buffer (pH 7.4), fixed in 1 % osmic acid solution for 2 h, and rinsed with 0.1M phosphate buffer (pH 7.4) again. After gradient concentration ethanol dehydration, the specimens underwent critical point drying (Quorum K850, UK) and were then sputter-coated with gold. Cross-sectional SEM images were acquired at an accelerating voltage of 10 kV.

2.3. Preparation of tdECM hydrogel

The decellularized tendons were ground into powder using a liquid nitrogen freezer grinder (SPEX SamplePrep 6875 Mill, USA). Following milling, the decellularized tendon tissues were subjected to digestion for 24 h in a solution containing 0.1 M Hydrochloric Acid (HCl) (Aladdin, Shanghai, China) and 2 mg/mL pepsin (Sigma-Aldrich, Germany). Subsequently, the digested solution was neutralized on ice to a pH of 7.4 using Sodium hydroxide (NaOH) (Aladdin, Shanghai, China) to form the hydrogel. The osmotic pressure of the hydrogel was adjusted to physiological levels by adding a 1:10 volume of 10 × phosphate buffer saline (PBS) (Servicebio, Wuhan, China). Temperature-mediated gelation was then initiated by incubating the hydrogel at 37 °C for 1 h.

2.4. Morphological characterizations of tdECM hydrogel

The microstructure of the tdECM hydrogel was examined using SEM (ZEISS Sigma300, Germany). Post-gelation, the hydrogel samples were subjected to freeze-drying (SCIENTZ-12N/A, Ningbo, China) for 48 h, followed by sputter coating with a thin layer of gold. Imaging was conducted with the SEM operated at an accelerating voltage of 3 kV and a working distance of 10.4 mm.

2.5. Swelling and degradation of tdECM hydrogel

To assess the swelling ratio (SR), 500 µl of tdECM hydrogel samples (n = 3/set time) were crosslinked at 37 °C and weighed (W₀), then

immersed in 1 × PBS at 37 °C. At designated times, the hydrogels were reweighed (W_t) after excess water was removed using wet tissue paper. The samples' swelling ratio was determined using the following equation: SR (%) = (W_t – W₀)/W₀ × 100 %.

The degradation rate of the tdECM hydrogel (n = 3/set time) was performed in 1 × PBS, with the initial weights of the hydrogels defined as W₀. The samples were placed in a shaker at 37 °C in PBS solution, and their dry weight was recorded after 1, 3, 7, 14, 21, and 28 days. The weight of the hydrogel at set time intervals was described as W_t. The degradation rate was calculated with the following equation: Degradation rate (%) = (W₀ – W_t)/W₀ × 100 %.

2.6. Injectable and mechanical characterizations of tdECM hydrogel

A mold with intricate geometry was utilized to evaluate the injection and fluidity characteristics of the hydrogel. The tensile property of the hydrogel was evaluated on a material tensile testing equipment (5943, Instron, USA). Three samples were immersed in PBS to achieve swelling equilibrium, after which the hydrogels were elongated at a continuous rate of 2 mm per minute until failure occurred. The viscosities of the tdECM hydrogel were assessed with a rotational viscometer (NDJ-8S, Hengping, China) (n = 5).

2.7. Isolation and identification of rabbit tendon-derived stem cells (TDSCs)

In this study, Achilles tendon tissue from six-week-old male rabbits was sectioned into small pieces and subjected to digestion for 2 h at 37 °C using 3 mg/mL type I collagenase (Beyotime, Shanghai, China). The resultant digested cells were then suspended in low-glucose Dulbecco's Modified Eagle Medium (LG-DMEM) supplemented with 10 % fetal bovine serum (FBS) (Gibco, USA) and 1 % penicillin/streptomycin (Beyotime, Shanghai, China). The culture medium was refreshed every 2 days. TDSCs were passaged upon reaching approximately 80 % confluency. Cells at passage 3 to 5 were utilized for subsequent experiments.

For identification of TDSCs, cells at passage 3 were incubated with the following conjugated antibodies: FITC-conjugated anti-CD44 (1:50; bs-0521R-FITC; Bioss), FITC-conjugated anti-CD34 (1:50; bs-2038R-FITC; Bioss), FITC-conjugated anti-CD45 (1:50; bs-0522R-FITC1; Bioss), APC-conjugated anti-CD90 (1:50; Cat No:561409; BD Biosciences). Flow cytometry analysis was conducted using a Beckman CytoFLEX flow cytometer (Beckman Coulter, USA), and the data were analyzed utilizing FlowJo software. The differentiation of TDSCs at passage 3 into osteocytes, adipocytes, and chondrocytes was evaluated using osteogenic, adipogenic, and chondrogenic induction medium. After 21 days, we performed Alizarin Red S, Oil Red O, and Toluidine Blue O.

2.8. Hydrogel biocompatibility

The hydrogel embedded with TDSCs was subjected to live/dead cell staining (KeyGEN BioTECH, Nanjing, China) and cytoskeleton staining (Xiaoyou, Hangzhou, China) at 1, 4, and 7 days post-inoculation to assess cell number and viability using a fluorescence microscope (OLYMPUS IX73P1F, Japan). Each sample was allocated three wells. Additionally, the hydrogel loaded with TDSCs underwent a CCK-8 cell proliferation assay (KeyGEN BioTECH, Nanjing, China) at 1, 3, and 7 days post-inoculation.

2.9. Isolation and identification of TDSCs-Exos

Upon reaching 80 % confluence, TDSCs were cultured in a medium supplemented with 10 % serum devoid of exosomes. After 24 h, the culture medium was collected and subjected to sequential centrifugation at 500×g for 5 min, 2000×g for 15 min, and 10,000×g for 45 min at 4 °C to eliminate cellular debris. The resultant supernatant was transferred to

a centrifugal filter tube (10 kDa; Millipore, USA) and centrifuged at $4000\times g$ for 20 min. Subsequently, the Quick Exosome Isolation Kit (Yeasen, Shanghai, China) was employed for incubation over 12 h, followed by centrifugation at $10,000\times g$ for 1 h to precipitate the exosomes. The total protein concentration of exosomes was quantified utilizing the Bicinchoninic Acid (BCA) Protein Assay Kit (Beyotime, Shanghai, China). The morphology and quality of the exosomes were assessed through transmission electron microscopy (TEM) (HITACHI HT7800, Japan), while the particle size distribution was determined via nanoparticle tracking analysis (NTA) (Malvern Panalytical NanoSight NS300, UK). Additionally, Western blot analysis was employed to detect the presence of exosomal surface markers CD63, TSG101, and Calnexin.

2.10. Uptake of TDSCs-Exos by TDSCs and macrophages

For the fluorescent labeling of TDSCs-Exos, a PKH67 solution (Solarbio, Beijing, China) was added to TDSCs-Exos and incubated according to the manufacturer's instructions. The mixture was then transferred to a centrifugal filter tube and centrifuged at $4000g$ at $4^\circ C$ for 30 min to remove excess dye. The PKH67-labeled Exo were subsequently incubated with TDSCs and Tohoku Hospital Pediatrics-1 (THP-1) for 6 h, fixed in 4 % paraformaldehyde (PFA) for 15 min, and stained with DAPI for 5 min. Finally, fluorescent images were captured using a confocal imaging system (Leica STELLARIS8, Italy).

2.11. MicroRNA sequencing

The preparation and sequencing of the miRNA library were conducted using a commercial service (LC-Bio Technology Co., Ltd, Hangzhou, China). In summary, total RNAs were extracted from TDSCs-Exos obtained from three independent batches. Subsequently, 3' and 5' RNA adapters were ligated to each end, followed by reverse transcription and PCR amplification. The PCR products were purified via gel electrophoresis and evaluated using the Agilent Technologies 2100 Bioanalyzer. The miRNA library was then constructed using the TruSeq Small RNA Sample Prep Kits (Illumina, San Diego, USA) and sequenced on the Illumina HiSeq 2500 platform.

The raw reads underwent processing with ACGT101-miR (v4.2) to generate clean reads, which were then mapped to the genome of the species using miRBase 22.1 through a BLAST search. To predict the genes targeted by the most abundant miRNAs, two computational target prediction algorithms (TargetScan, v5.0 and Miranda, v3.3a) were used to identify miRNA binding sites. Then, the data predicted by both algorithms were combined and the overlaps were calculated. The Gene Ontology (GO) terms and Kyoto Encyclopedia of Genes and Genomes (KEGG) Pathway of these most abundant miRNAs and their targets were annotated as well. GO and KEGG enrichment analyses were performed using R software package, with $p < 0.05$ as the significance criteria.

2.12. The effects of TDSC-Exos on TDSCs in vitro

The impact of exosomes on cell proliferation was evaluated using the CCK-8 assay. In brief, TDSCs were seeded at a density of 2×10^3 cells per well in 96-well plates. Various concentrations of TDSCs-Exos (0, 25, 50, 100 $\mu g/mL$) were administered and incubated with the TDSCs. At 1, 3, and 7 days post-incubation, the culture medium was replaced with 110 μL of LG-DMEM containing 10 μL of CCK-8 reagent. The cells were then incubated for an additional 2 h at $37^\circ C$. Absorbance was measured at 450 nm using a microplate reader (Molecular Devices, USA).

The migration ability of TDSCs was evaluated using the scratch test and transwell assay. For the scratch test, TDSCs were seeded at a density of 1×10^5 cells per well in six-well plates. A linear cell-free area was created by scratching the monolayer with the tip of a 200 μL pipette. Following a PBS wash, media containing varying concentrations of exosomes (0, 25, 50, 100 $\mu g/mL$) was added. The wound-healing process was documented through microscopic imaging at 0 h and 24 h.

For the transwell assay, TDSCs were seeded at a density of 4×10^4 cells per well into the upper chamber of a 24-well transwell plate (NEST; pore size: 8 μm). Concurrently, 600 μL of medium containing varying concentrations of exosomes (0, 25, 50, 100 $\mu g/mL$) was added to the lower chamber. After an incubation period of 24 h, the cells that had migrated to the underside of the membrane were fixed using 4 % paraformaldehyde and subsequently stained with 1 % Crystal Violet for 30 min. The number of migrated cells on the underside of the membrane was then quantified using microscopy.

Real-time quantitative PCR (RT-qPCR) was employed to evaluate the tendinogenic differentiation and anti-inflammatory effects of exosomes (0, 25, 50, 100 $\mu g/mL$) on specific gene expression in TDSCs. In summary, TDSCs were cultured in media containing varying concentrations of exosomes (0, 25, 50, 100 $\mu g/mL$) for a duration of 7 days. Subsequently, total cellular RNA was extracted from the cells using an RNA Extraction Kit (Accurate Biology, Changsha, China). Reverse transcription was conducted to generate cDNA libraries utilizing the ABScript III RT Master Mix for qPCR with gDNA Remover (ABclonal, Wuhan, China). Subsequent RT-qPCR was carried out using the SYBR Green Fast qPCR Mix (ABclonal, Wuhan, China) on a CFX96 Deep Well Real-Time system (BIO-RAD Laboratories, Hercules, CA, USA). The relative mRNA expression levels of collagen type I (COL1), tenascin C (TNC), and tenomodulin (TNMD) were normalized to GAPDH and quantified using the $2^{-\Delta\Delta CT}$ method. The primary sequences employed are detailed in Supplemental Table 1.

To investigate the anti-inflammatory effects of TDSCs-Exos, we cultured TDSCs in a medium containing 10 ng/mL Interleukin-1 β (IL-1 β) (ABclonal, Wuhan, China) and varying concentrations of exosomes (0, 25, 50, 100 $\mu g/mL$) for 24 h. Subsequently, we employed the established RT-qPCR method to quantify the relative mRNA transcription levels of COL1, IL-1 β , IL-6, and MMP3. The sequences of the primers utilized are provided in Supplemental Table 1.

2.13. Release profile of Exo in tdECM hydrogel

The tdECM hydrogel was prepared by incorporating 100 $\mu g/mL$ of exosomes and subsequently placed in a 48-well plate containing 200 μL of PBS. At specified time points (days 1, 2, 3, 7, and 14), half of the PBS was collected and replaced with 100 μL of fresh PBS. The concentration of exosomes released into the PBS was quantified using the BCA Protein Assay Kit (Beyotime, Shanghai, China).

2.14. Responses of TDSCs to the tdECM hydrogel with TDSCs-Exos in vitro

The proliferation of TDSCs was assessed utilizing the CCK-8 assay, following established protocols. The tdECM hydrogel, with or without TDSCs-Exos loaded with TDSCs, was subjected to proliferation assays at 1, 3, and 7 days post-inoculation. TDSCs cultured without the tdECM hydrogel and TDSCs-Exos served as the control group.

The impact of tdECM hydrogel and tdECM hydrogel with TDSCs-Exos (Exo-tdECM) on the migration of TDSCs in vitro was evaluated using the transwell assay and scratch test. The tdECM hydrogel, with or without 100 $\mu g/mL$ Exo, was introduced into the upper chamber of a 24-well transwell plate and subjected to thermal crosslinking at $37^\circ C$. Subsequently, 4×10^4 TDSCs per well were seeded in the lower chamber of the 24-well transwell plate. Upon reaching 80 % confluence, a straight line was created using the tip of a P200 pipette. After washing the wells, images of each group were captured at 0 and 24 h post-scratch using microscopy.

For the transwell assay, 4×10^4 cells were seeded into the upper chamber of a 24-well transwell plate. Subsequently, culture medium was added to the tdECM hydrogel in the lower chamber, with or without 100 $\mu g/mL$ TDSCs-Exos (Fig. 4b). Following a 24-h incubation period, the cells were fixed using 4 % paraformaldehyde and stained for 30 min with 1 % crystal violet. Cells on the upper surface of the membranes were

removed. Migratory activity was quantified by counting the number of cells that had migrated.

RT-qPCR was performed to evaluate the tendinogenic differentiation and anti-inflammatory effects of Exo-tDECm on specific gene expression in TDSCs. As previously described, after a 7-day co-culture of the cells with either the tDECm hydrogel or Exo-tDECm, RNA was extracted and reverse-transcribed into complementary DNA (cDNA). Subsequently, RT-qPCR was conducted to quantify the relative mRNA transcription levels of COL1, TNC, and TNMD. Additionally, TDSCs were co-cultured with medium containing 10 ng/mL IL-1 β and either the tDECm hydrogel or Exo-tDECm for 24 h. Subsequently, the established RT-qPCR methodology was employed to quantify the relative mRNA transcription levels of COL1, IL-1 β , IL-6, and MMP3 expression. The sequences of the primers in the study are listed in [Supplemental Table 1](#).

Cell immunofluorescence assays were employed to assess the impact of tDECm hydrogel and Exo-tDECm on tendinogenic differentiation. Specifically, after a 7-day co-culture period with either tDECm hydrogel or Exo-tDECm, TDSCs were fixed with 4 % PFA for 20 min and subsequently washed three times with PBS. The cells were then permeabilized using 0.1 % Triton X-100 for 10 min and blocked with BSA for 1 h. Subsequently, the primary antibodies targeting Collagen I (1:200; bs-10423R; Bioss), TNMD (1:200; bs-7525R; Bioss), and TNC (1:200; bs-1327R; Bioss) were incubated at 4 °C overnight. This was followed by incubation with a secondary antibody (1:500; SA00013; Proteintech) for 1 h at room temperature. After triple washing with PBS, the nuclei were stained with DAPI for 5 min. Finally, the cells were examined using a fluorescence microscope.

2.15. Effect of the tDECm hydrogel and Exo-tDECm on the inflammatory response *in vitro*

In summary, THP-1 cells were seeded at a density of 5×10^5 cells per well and co-cultured with either LPS + tDECm or LPS + Exo-tDECm. For the control group, 5×10^5 cells were stimulated with PMA and LPS to induce M0 and M1 activation, respectively. After 48 h of co-culture, the THP-1 cells were analyzed to assess the immunomodulatory properties of the tDECm hydrogel and Exo-tDECm using immunofluorescence staining, RT-qPCR, flow cytometry, and Enzyme-Linked Immunosorbent Assay (ELISA).

For immunofluorescence staining, cells were fixed with PFA for 20 min and permeabilized with 0.1 % Triton X-100 for 10 min at room temperature. This was followed by a blocking step using 5 % (w/v) BSA for 1 h. Subsequently, cells were incubated overnight at 4 °C with primary antibodies against CD86 (1:200; 13395-1-AP; Proteintech) and CD206 (1:500; 18704-1-AP; Proteintech). After the overnight incubation, secondary antibodies (1:500; SA00013&SA00007; Proteintech) were applied, followed by DAPI staining. Images were captured using a confocal imaging system (Leica, Milan, Italy) and further processed with ImageJ software.

For RT-qPCR analysis, total RNA was extracted from THP-1 cells and subsequently reverse-transcribed into cDNA. Quantitative PCR (qPCR) was then conducted to assess the relative mRNA transcription levels of CD86, CD206, TNF- α , IL-6, and IL-10. The expression levels were normalized to β -Actin, and the relative expression levels were calculated using the $2^{-\Delta\Delta CT}$ method. The sequences of the primers in the study are listed in [Supplemental Table 1](#).

Flow cytometry analysis was employed to assess macrophage polarization. THP-1 cells were harvested and prepared as single-cell suspensions. Subsequently, the cells were incubated with anti-CD86 antibodies (1:50; A26126; Abclonal) and anti-CD206 antibodies (1:50; 2,740,390; Thermo Fisher Scientific). Flow cytometry analysis was conducted using a Beckman CytoFLEX flow cytometer (Beckman Coulter, USA), and the data were analyzed utilizing FlowJo software.

To assess the concentrations of TNF- α , IL-6, and IL-10 in the supernatants of THP-1 cells subjected to various interventions, ELISA was conducted. Following a 48-h treatment with PMA, LPS, LPS + tDECm, or

LPS + Exo-tDECm as previously described, the culture medium was collected to determine the concentrations of TNF- α , IL-6, and IL-10. These concentrations were measured using the Human TNF-alpha ELISA Kit (Servicebio, Wuhan, China), Human IL-6 Uncoated ELISA (Thermo Fisher Scientific, USA), and Human IL-10 Uncoated ELISA (Thermo Fisher Scientific, USA), in accordance with the manufacturers' instructions. Absorbance at 450 nm was recorded using a microplate reader (Thermo Fisher Scientific, USA).

2.16. Animal experiments

To investigate the therapeutic efficacy of tDECm hydrogel and TDSCs-Exos in the treatment of tendinopathy, we developed a rabbit model of the condition. In order to investigate the release efficiency of TDSCs-Exos from tDECm hydrogel *in vivo*, we selected a rat Achilles tendon model. All experimental procedures received approval from the Laboratory Animal Welfare and Ethics Review Committee of Zhejiang University (Approval Number: ZJU20240230) and the Tab of Animal Experimental Ethical Inspection of the First Affiliated Hospital, Zhejiang University School of Medicine (Approval Number: 20,241,705). Male New Zealand White Rabbits (2.5–3 kg) were procured from Fuyang Hongfeng Rabbit Company. Sprague-Dawley (SD) rats (450–500g) were purchased from Hangzhou Medical College.

To assess the sustained release of exosomes encapsulated in the tDECm hydrogel *in vivo*, DiR-labeled TDSCs-Exos (100 μ g/50 μ L PBS or tDECm) were locally injected into the left Achilles tendon tissues of six rats ($n = 3$ per group, with an injection volume of 50 μ L). A live imaging system (Photon IMAGER Optima; Biospace Lab, France) was employed to observe the left leg of rats at 1, 3, 7, and 14 days following injection.

A total of 18 male New Zealand White Rabbits were used for *in vivo* experiments. The rabbit tendinopathy model was established by a single injection of collagenase type I according to previous studies [29,30]. Following the administration of anesthesia to the animals, a 29-gauge needle was inserted into the Achilles tendon at a point 5 mm proximal to the calcaneus. The needle was advanced longitudinally along the tendon axis for approximately 10 mm. Subsequently, an intratendinous injection of 110 μ L of type I collagenase/hydrogel/saline solution was performed, accompanied by the gradual retraction of the needle. Specifically, 110 μ L of collagenase type I (125 U/mg, 2.4mg/rabbit) was administered via injection into the Achilles tendon tissues. One week later, male New Zealand White rabbits ($n = 6$ /group, 12 legs/group) were randomly and averagely assigned to receive an injection of either saline (110 μ L), tDECm hydrogel (110 μ L), or Exo-tDECm (110 μ L) in the Achilles tendon region. Following the injection, all rabbits were allowed unrestricted cage activity. At 3 and 6 weeks post-injection, all rabbits were euthanized, and their tendons were harvested for subsequent experimental analyses.

2.17. Histology and immunostaining

Tendon specimens ($n = 3$ /group) from different rabbits excised at 3 and 6 weeks post-surgery were fixed in 4 % paraformaldehyde, embedded in paraffin, and longitudinally sectioned to a thickness of 5 μ m. Subsequently, the samples were stained with H&E, and Masson's trichrome, following standard protocols. Tissue morphology was examined using a digital pathology section scanner (3DHISTECH P25VFLASH, Hungary). Semi-quantitative histological analysis was performed using the Bonar scoring system, as previously described [31].

For immunohistochemistry, tissue sections were deparaffinized, blocked, and incubated overnight at 4 °C with the following primary antibodies: anti-TNC, anti-TNMD, anti-iNOS (1:200; bs-2072R; Bioss), anti-ARG1 (1:200; bs-23837R; Bioss), anti-IL-6 (1:200; bs-6312R; Bioss), and anti-IL-10 (1:200; bs-0698R; Bioss). Subsequently, the sections were incubated with secondary antibodies (1:500; SA00013&SA00007; Proteintech) for 1 h at 37 °C, followed by staining with DAPI solution. Visualization was performed using an immunofluorescence microscope.

2.18. Gait analysis

A 100 × 30 cm track was designed for rabbits (n = 3/group) with red hind paws to walk freely from one side to the other. We recorded their tracks and analyzed average stride length at 6 weeks.

2.19. Biomechanical test

At 6 weeks post-intervention, the biomechanical properties of tendon specimens (n = 3 per group) collected from different rabbits were evaluated using a biomechanical testing device (5943, Instron, USA). Following the removal of excess tissue from the tendon-bone complex, the diameters and lengths of the specimens were accurately measured with a caliper. Subsequently, the specimens were firmly attached to the

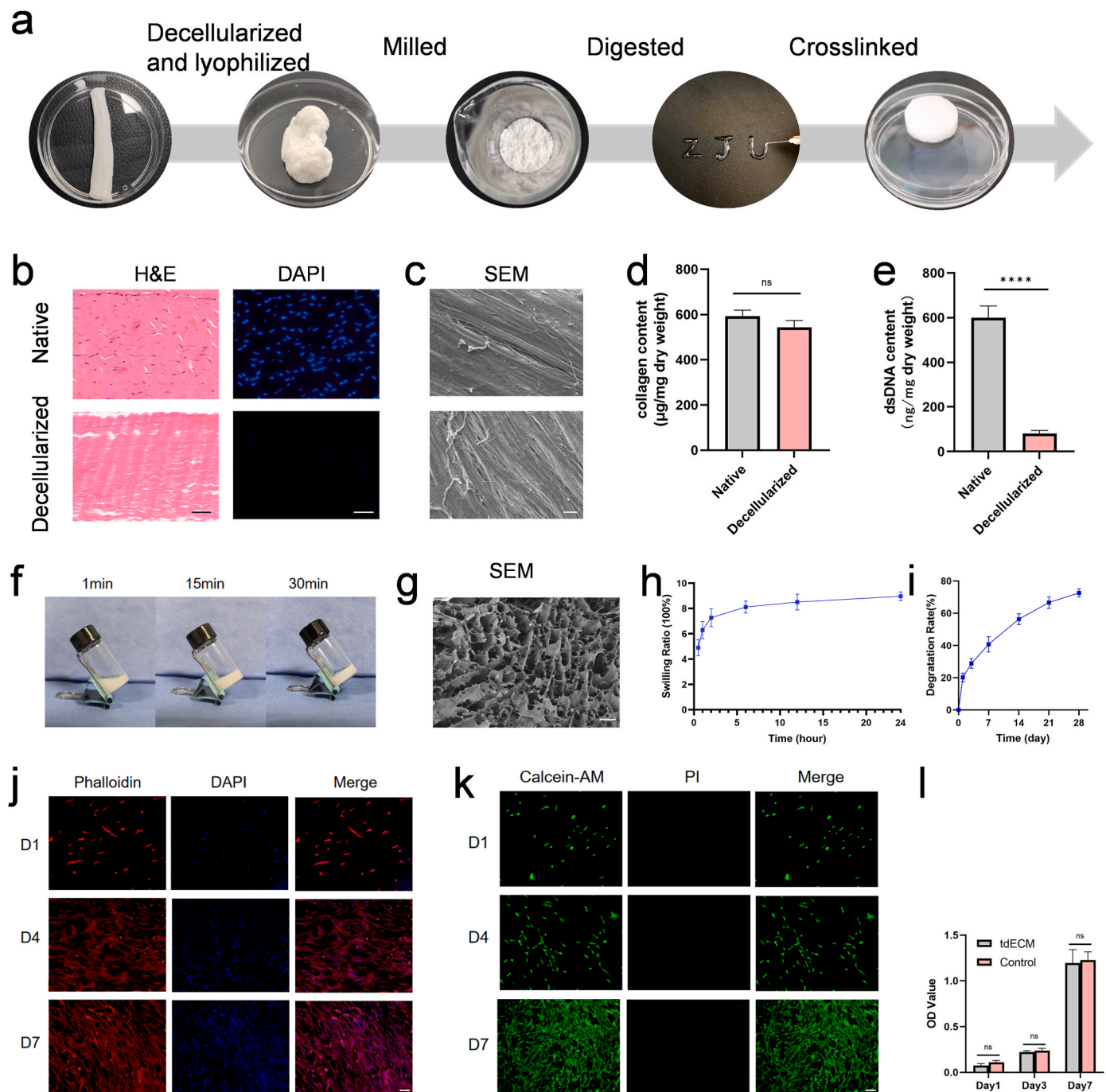


Fig. 2. Characterization of decellularized tendon and tDECm hydrogel. (a) A process for the preparation of tDECm hydrogel. (b) H&E and DAPI staining on native and decellularized tendon sections. Scale bar = 50 µm. (c) SEM on the native and decellularized tendon. Scale bar = 10 µm. (d, e) Collagen content and dsDNA content, normalized to dry weight of tissue for the native and decellularized tendon (n = 3/group). (f) tDECm hydrogel crosslinking degree at different times of 37 °C. (g) SEM on tDECm hydrogel. Scale bar = 200 µm. (h–i) Swelling and degradation rate of tDECm hydrogel (n = 3). (j) Cytoskeleton and DAPI staining of TDCs seeded on the tDECm hydrogel at 1, 4, and 7 days by fluorescence microscopy (red, cytoskeleton; blue, nucleus). Scale = 100 µm. (k) Live/Dead staining of TDCs seeded on the tDECm hydrogel at 1, 4, and 7 days by fluorescence microscopy (green, live cells; red, dead cells). Scale = 100 µm. (l). Proliferation of TDCs in tDECm hydrogel and control group was assessed by CCK-8 (n = 3/group). *P < 0.05, **P < 0.01, ***P < 0.001, ****P < 0.0001, vs. control group.

upper and lower clamps of the testing apparatus. The tendons underwent a tensile load at a steady extension rate of 5 mm/min until failure ensued. The mechanical properties were evaluated by measuring the real-time load and displacement. The failure load was defined as the peak load recorded during testing. The Young's modulus was calculated from the slope of the linear part of the stress-strain curve.

2.20. Statistical analysis

All experiments were performed using at least three independent samples. Statistical analyses were performed using GraphPad Prism 9 Software (CA, USA). Data are presented as mean \pm standard deviation. Comparisons between the two groups were conducted using the Student's t-test. For multiple group comparisons, one-way ANOVA followed by Tukey's post hoc test was employed. Statistical significance was defined as $P < 0.05$, with significance levels indicated as * $P < 0.05$, ** $P < 0.01$, and *** $P < 0.001$.

3. Results

3.1. Fabrication and characterizations of tdECM hydrogel

Before preparing the tdECM hydrogel, the Porcine Achilles tendons underwent a thorough decellularization process (Fig. 2a). H&E staining of the tendons, both pre- and post-decellularization, revealed that the native collagen structure of the tendon was preserved while cellular components were effectively removed (Fig. 2b). Additionally, DAPI staining confirmed the absence of nuclei in the decellularized tendon tissue (Fig. 2b). In contrast, a substantial presence of nuclear material was observed in the native tendon. The structural composition and integrity of both native and decellularized tendon tissue samples were evaluated using SEM (Fig. 2c). The analysis revealed that both types of tissue samples consisted of collagen fibers, with the native tissue exhibiting a more organized arrangement. No chemical crystals were observed in the decellularized tissue, indicating the thorough removal of detergents utilized during the decellularization process. The preservation of the fibrous structure in both samples further corroborates the effectiveness of the decellularization procedure.

The DNA quantification assay revealed a substantial reduction in residual DNA content in the decellularized tendon tissue (80.33 ± 14.29 ng/mg) compared to the native tendon tissue (599.67 ± 53.27 ng/mg), thereby demonstrating the effective removal of DNA from the native tendon (Fig. 2e). Hyp is one of the main components of collagen, accounting for approximately 13.4 % of its composition, and is widely regarded as a distinctive amino acid within the collagen structure. The presence of collagen was qualitatively assessed by measuring the amount of HYP (Fig. S1a). The study revealed that the residual collagen content in decellularized tissue (543.4 ± 30.49 μ g/mg) was comparable to that in native tissue (593.7 ± 25.82 ng/mg) (Fig. 2d). Statistical analysis indicated no significant difference between the two groups ($p > 0.05$), suggesting that the collagen content was preserved in both native and decellularized tendon tissues. These findings demonstrate that the optimized decellularization protocol effectively retains collagen content while removing cellular dsDNA.

A typical process for the production of tdECM hydrogel is illustrated in Fig. 2a, which also demonstrates that the tdECM hydrogel is injectable through a syringe equipped with a 26-gauge needle. Utilizing a mold with complex geometry, our research revealed that the tdECM hydrogel had excellent injectability and fluidity before crosslinking, and achieved an ideal viscosity post-crosslinking (Fig. S1b). The neutralized pre-gel transitions from a liquid to a solid state after incubation at 37 °C and exhibits no flow behavior after 15 min at this temperature, confirming its crosslinking (Fig. 2f). Furthermore, SEM analysis revealed that the microstructure of the hydrogel is characterized by an interconnected and highly porous architecture (Fig. 2g).

The swelling ratio of hydrogel is crucial for the exchange of nutrients

and fluids between the body and its environment. The swelling ratio shown in Fig. 2h indicates that the hydrogel has a nutrient and fluid permeability with time. The rate at which the hydrogel samples degraded was also depicted over time (Fig. 2i). On day 28, the hydrogel preserved approximately 27 % of its initial mass. The tdECM hydrogel exhibits an elastic modulus of 4.35 ± 0.56 kPa and a viscosity of 2925 ± 46.44 mPa s.

Regarding the biocompatibility of hydrogels, a comparison between the normal group without tdECM hydrogel and the group with the hydrogel loaded with TDSCs revealed no significant differences in the CCK-8 proliferation assay on days 1, 3, and 7, indicating robust cell proliferation performance of the tdECM hydrogel (Fig. 2l). Cytoskeleton and live/dead cell staining at various time points further demonstrated that the tdECM hydrogel exhibits good biocompatibility with TDSCs (Fig. 2j and k). On day 1, the number of cells on the hydrogel was low, the cytoskeleton was not fully developed, and there were few dead cells. Over time, TDSCs continued to exhibit a low mortality rate, while the skeletal structure demonstrated substantial expansion and proliferation.

3.2. Characterization of TDSCs and TDSCs-Exos

Flow cytometric analysis and differentiation results verify that the cells derived from tendons were stem cells. The data indicated the presence of CD90 (98.3 %) and CD44 (99.7 %), which are classic markers of stem cells, while CD45 and CD34, markers for leukocytes and hematopoietic stem cells, were absent. It was established that TDSCs can successfully transform into osteogenic, adipogenic, and chondrogenic cells in vitro induction medium (Fig. S2).

TEM revealed that the TDSCs-Exos exhibited spherical vesicles with bilayer membranes, approximately 100 nm in diameter (Fig. 3a). NTA further confirmed a similar particle size distribution, with a mean diameter of 105 nm (Fig. 3b). Western blot analysis indicated the presence of exosomal surface markers CD63 and TSG101, while the endoplasmic reticulum protein Calnexin was absent (Fig. 3c). Additionally, exosomes labeled with the PKH67 fluorescent dye were observed to localize around the cell nucleus, suggesting the internalization of TDSCs-Exos by TDSCs and THP-1 (Fig. 3e). These characteristics are consistent with findings from previous studies of exosomes [32, 33].

To investigate the impact of exosomes on TDSCs and determine the optimal concentration, we initially examined the proliferation and migration capabilities of TDSCs exposed to varying concentrations of exosomes (0, 25, 50, 100 μ g/mL). The results from the CCK-8 proliferation assay indicated that exosomes at different concentrations enhanced TDSC proliferation at various time points, with the 100 μ g/mL concentration exhibiting the most pronounced effect (Fig. 3d). Additionally, both scratch and transwell assays, which assess cellular migration, demonstrated similar trends in response to the exosome concentration gradients. The Transwell assay demonstrated a positive correlation between the concentration of exosomes applied to TDSCs and the number of cells traversing the membrane over a 24-h period (Fig. 3f and g). In the scratch assay, the 100 μ g/mL exosomes intervention group exhibited the highest cell migration (Fig. 3h and i).

We employed RT-qPCR to assess the impact of varying exosome concentrations on the tendon differentiation of TDSCs. The results indicated that the expression levels of COL1, TNC, and TNMD were significantly elevated on day 7 in the group treated with 100 μ g/mL of exosomes. In comparison to the 0 μ g/mL exosomes group, although the mRNA levels of tendon differentiation-related markers were also enhanced in the group treated with 25 μ g/mL of exosomes for 7 days, this increase did not reach statistical significance (Fig. 3j–l).

To investigate the anti-inflammatory effects of exosomes on inflammatory TDSCs, we co-cultured TDSCs with varying concentrations of exosomes and IL-1 β for 24 h. Subsequently, cells were harvested for RT-qPCR analysis. The results indicated that exosomes at a concentration of 100 μ g/mL exhibited a superior anti-inflammatory effect, as

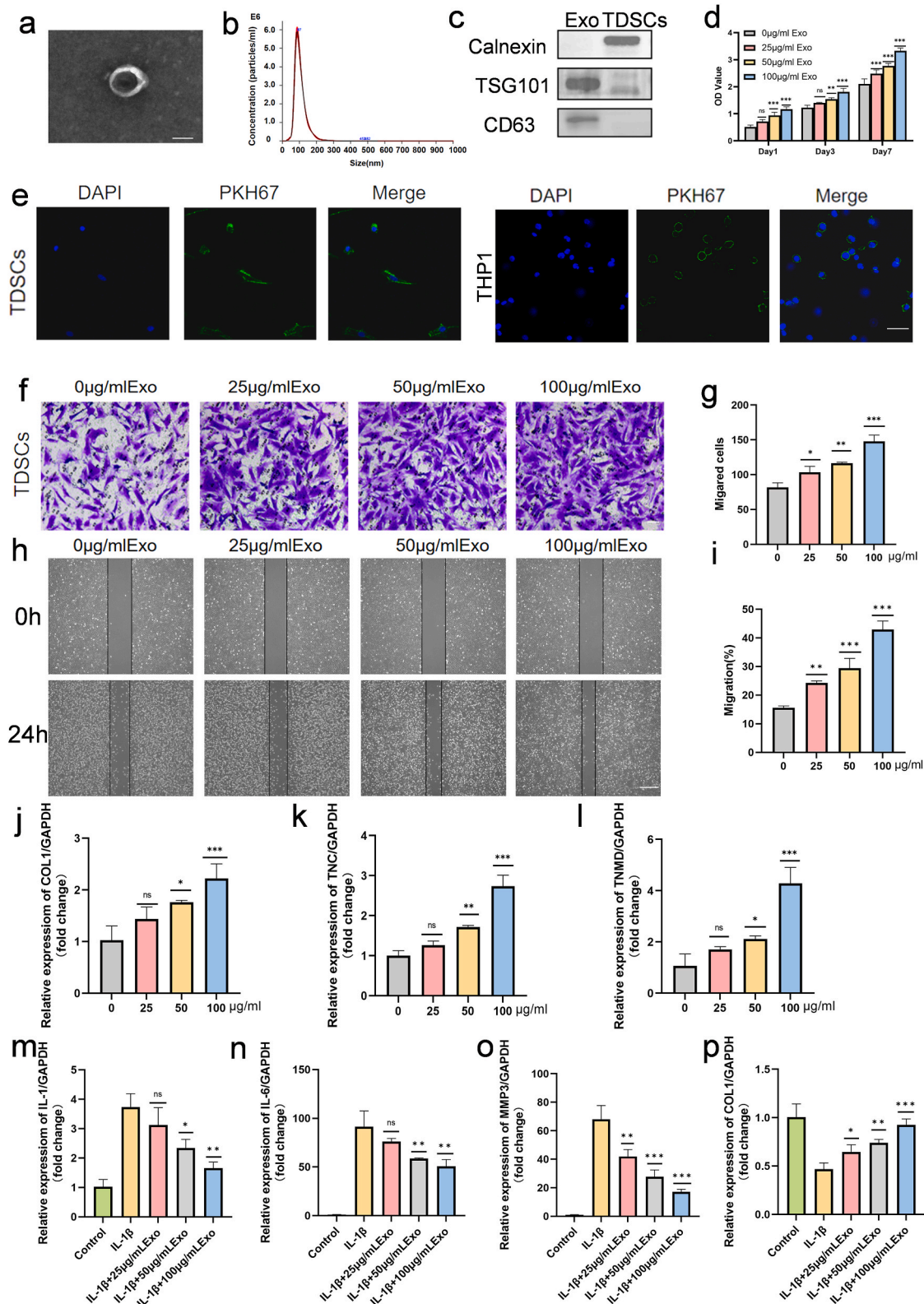


Fig. 3. Characterization of TDSCs-Exos. (a) Morphology of TDSCs-Exos measured by TEM. Scale bar = 100 nm. (b) Particle size distribution of TDSCs-Exos examined by NTA. (c) Western blot analysis of TDSCs-Exos surface markers CD63, TSG101, and Calnexin. (d) The proliferation of TDSCs treated with different concentrations of TDSCs-Exos measured by CCK-8 (n = 3/group). (e) Fluorescent images of PKH67-labeled TDSCs-Exos taken up by TDSCs and THP-1. Scale bar = 50 µm. (f,g) The migration of TDSCs treated with different concentrations of Exo assessed by transwell assay (n = 3/group). Scale bar: 50 µm. (h, i) The migration of TDSCs treated with different concentrations of TDSCs-Exos detected by scratch assay (n = 3/group). Scale bra = 500 µm. (j–l) COL1, TNC, TNMD relative mRNA level of TDSCs treated with different concentrations of TDSCs-Exos assessed by RT-qPCR (n = 3/group). (m–p) IL-1β, IL-6, MMP3, COL1 relative mRNA level of TDSCs treated with different concentrations of TDSCs-Exos assessed by RT-qPCR (n = 3/group). *P < 0.05, **P < 0.01, ***P < 0.001 vs. control group.

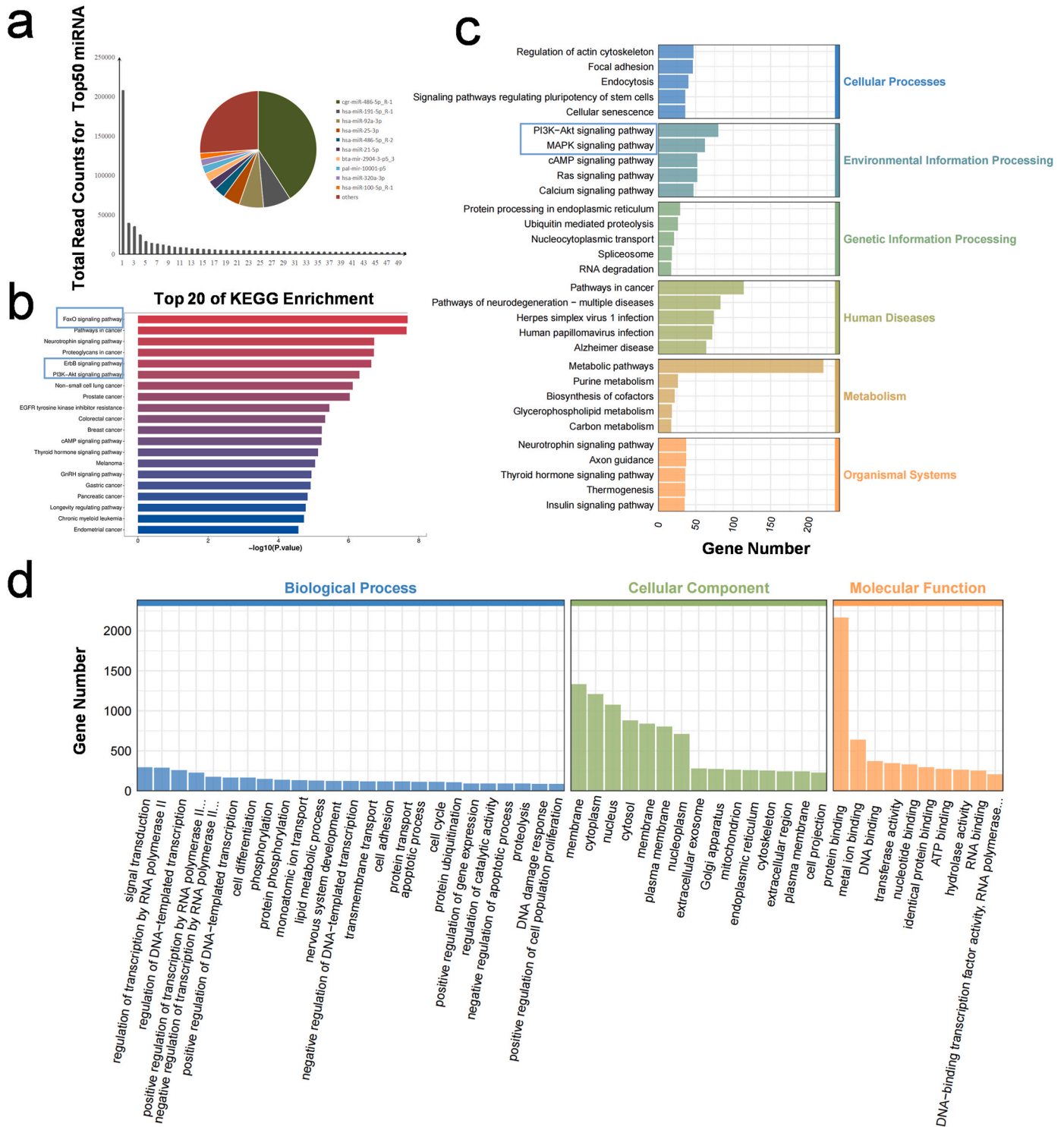


Fig. 4. miRNA sequencing and bioinformatic analyses. (a) Top 50 miRNA read counts in TDCs-Exos. (b–c) KEGG analysis determined the most related signaling pathways of miRNAs in TDCs-Exos. (d) GO analysis of miRNAs in TDCs-Exos.

evidenced by the reduced mRNA levels of IL-1 β , IL-6, and MMP3. Additionally, exosomes at this concentration were able to restore the COL1 mRNA levels, which had been diminished due to inflammation, back to normal levels. The mRNA levels of IL-1 β and IL-6 in the 25 μ g/mL exosome intervention group did not exhibit statistically significant differences compared to the IL-1 β stimulation group alone. However, the expression of MMP3 and COL1 in the 25 μ g/mL exosome intervention group was significantly enhanced (Fig. 3m–p). Consequently, the anti-inflammatory and tendinogenic effects of 100 μ g/mL exosomes were

superior to those observed with 0, 25, and 50 μ g/mL exosomes. Therefore, a concentration of 100 μ g/mL was selected for subsequent experiments.

3.3. miRNA sequencing in TDCs-Exos

To investigate the role of miRNAs in the regulation of tendon repair by TDCs-Exos, we conducted miRNA sequencing on TDCs-Exos. The sequencing results identified the top 10 enriched miRNAs in TDCs-Exos

as follows: miR-486-5p_R-1, miR-191-5p_R-1, miR-92a-3p, miR-25-3p, miR-486-5p_R-2, miR-21-5p, mir-2904-3-p5_3, mir-10001-p5, miR-320a-3p, and miR-100-5p_R-1 (Fig. 4a).

The KEGG analysis indicated that these miRNAs were predominantly associated with metabolic pathways. Notably, the PI3K-Akt signaling pathway and the MAPK signaling pathway were the most enriched concerning environmental information processing (Fig. 4c). The top 10 KEGG enrichment pathways encompass the FoxO signaling pathway, PI3K-Akt signaling pathway, and ErbB signaling pathway, each of which is associated with cell proliferation and migration [34–36] (Fig. 4b). According to the GO analysis (Fig. 4d), the miRNAs were predominantly associated with protein binding, metal ion binding, and DNA binding within the context of molecular functions. In terms of cellular components, the membrane exhibited the highest level of enrichment. Regarding biological processes, the miRNAs were linked to signal transduction, transcription, and cell differentiation.

3.4. Release profile of TDSCs-Exos in tdECM hydrogel

To evaluate the release efficiency of exosomes from tdECM hydrogel, quantitative slow-release solutions were collected at various time points and analyzed using the BCA Protein Assay. The cumulative release of exosomes was then calculated. The data indicate that the highest release of exosomes occurs on the first day, accounting for up to 35 % of the total amount. Subsequently, the release efficiency of exosomes gradually declines. By the 14th day, the cumulative release volume exceeds 90 % (Fig. 5a).

3.5. Effect of tdECM hydrogel and Exo-tdECM on cellular behavior of stem cells in vitro

The CCK-8 proliferation assay demonstrated that, with the exception of the first day, the Exo-tdECM group exhibited significantly enhanced cell proliferation compared to both the tdECM group and the control group on days 4 and 7 (Fig. 5c). Additionally, the conditioned medium from the Exo-tdECM group more effectively promoted the migration of TDSCs than that from the tdECM group and the control group, as evidenced by the transwell and scratch assays (Fig. 5d–e,g,k). In summary, these findings indicate that while tdECM alone possesses the capability to promote cell proliferation and migration, the inclusion of exosomes further amplifies these effects.

Through RT-qPCR and immunofluorescence assays, it has been demonstrated that tdECM facilitates the tendinogenic differentiation of TDSCs at both the mRNA and protein levels. This is evidenced by the increased expression of the markers COL1, TNC, and TNMD. Notably, these markers exhibited higher expression levels in TDSCs cultured with Exo-tdECM (Fig. 5f,h-j,l-n).

Subsequently, we investigated the role of tdECM and TDSCs-Exos in modulating the inflammatory response of TDSCs in vitro. In the inflammation-induced TDSC model, RT-qPCR analysis demonstrated that a 24-h stimulation with IL-1 β significantly upregulated the expression of inflammation-related markers IL-1, IL-6, and MMP3, while concurrently leading to a marked downregulation of COL1, the primary collagen in tendons. The concurrent administration of tdECM during the intervention resulted in a significant reduction in the expression levels of IL-1, IL-6, and MMP3, while the expression of COL1 was moderately enhanced; however, these changes did not reach statistical significance when compared to the group stimulated solely with IL-1 β (Fig. 5o–r). The figures indicate that the supplementary exosome treatment amplifies the anti-inflammatory effects and collagen restoration properties of tdECM, demonstrating statistically significant differences relative to the IL-1 β stimulated group.

3.6. Exo-tdECM regulate M1 macrophages towards M2 macrophages in vitro

To further elucidate the regulatory effects of Exo-tdECM on macrophage repolarization, this study utilized the widely employed THP-1 macrophage cell line. Initially, THP-1 cells were differentiated into M0 phenotype macrophages via PMA induction for 24 h, followed by polarization into M1 phenotype macrophages through LPS stimulation for 48 h. The phenotypic alterations in macrophages were assessed by introducing tdECM or Exo-tdECM in conjunction with LPS stimulation. RT-qPCR analysis demonstrated that LPS effectively induced the upregulation of proinflammatory markers CD86, IL-6, and TNF α , while significantly downregulating the expression of anti-inflammatory markers CD206 and IL-10 (Fig. 6a–e). Treatment with tdECM resulted in a reduction in the expression of proinflammatory markers and an increase in the expression of anti-inflammatory markers. Furthermore, the addition of TDSCs-Exos treatment potentiated the effects of tdECM treatment.

Furthermore, we conducted immunofluorescence staining to assess the expression of M1 and M2 macrophage markers, aiming to investigate phenotypic changes in THP-1 macrophages subjected to tdECM or Exo-tdECM interventions. The results indicate that tdECM treatment inhibited M1 polarization while promoting M2 polarization of macrophages. In comparison to the LPS and LPS + tdECM groups, the LPS + Exo-tdECM group exhibited a significant reduction in M1 macrophages and a significant increase in M2 macrophages (Fig. 6f–h).

Flow cytometry analysis demonstrated that treatment with additional exosomes significantly reduced the CD86-positive rate, indicative of M1 macrophages, compared to the LPS and LPS + tdECM groups (Fig. 6i and j). Conversely, the percentage of CD206-positive cells, representing M2 macrophages, increased following LPS + Exo-tdECM treatment (Fig. 6k and l).

Based on the ELISA analysis, the results indicated that intervention with either tdECM or Exo-tdECM significantly suppressed LPS-induced secretion of IL-6 and TNF α in macrophages, while concurrently increasing the concentration of the anti-inflammatory factor IL-10 (Fig. 6m–o).

Collectively, these findings indicate that tdECM treatment effectively induces a phenotypic shift in THP-1 cells from M1 macrophages to M2 macrophages. Furthermore, the supplementary TDSCs-Exos treatment amplifies the effects of tdECM treatment.

3.7. Exo-tdECM promotes Achilles tendon repair in vivo

The tdECM hydrogel functions effectively as a sustained-release system, facilitating the continuous release of TDSCs-Exos for a minimum duration of two weeks in vitro. Additionally, DIR-labeled TDSCs-Exos were injected directly into the tendons of rats, and their retention was evaluated using the Photon Imager Optima on days 1, 3, 7, and 14. Compared to the group administered Exo alone, the tdECM-Exo cohort demonstrated a significantly more intense fluorescence signal at each time point after injection, suggesting that the hydrogel substantially improved the in vivo retention duration of TDSCs-Exos (Figs. S3a and b).

To examine the impact of Exo-tdECM on tendinopathy in vivo, we developed an Achilles tendon tendinopathy model using New Zealand rabbits (Fig. 7a). The administration of type I collagenase induced swelling, degeneration, and adhesion to surrounding tissues in the Achilles tendon. These pathological changes were mitigated by subsequent injections of tdECM hydrogel or Exo-tdECM. At 3 and 6 weeks post-treatment, H&E and Masson's trichrome staining analyses demonstrated that the Exo-tdECM injection significantly mitigated tendon fiber disorganization and reduced inflammatory cell infiltration to a greater extent than saline injection, with tdECM injection showing intermediate effects. These findings suggest that both tdECM and exosomes possess the potential to reverse tendon degeneration (Fig. 7b and c).

Furthermore, immunofluorescence analysis revealed a significantly

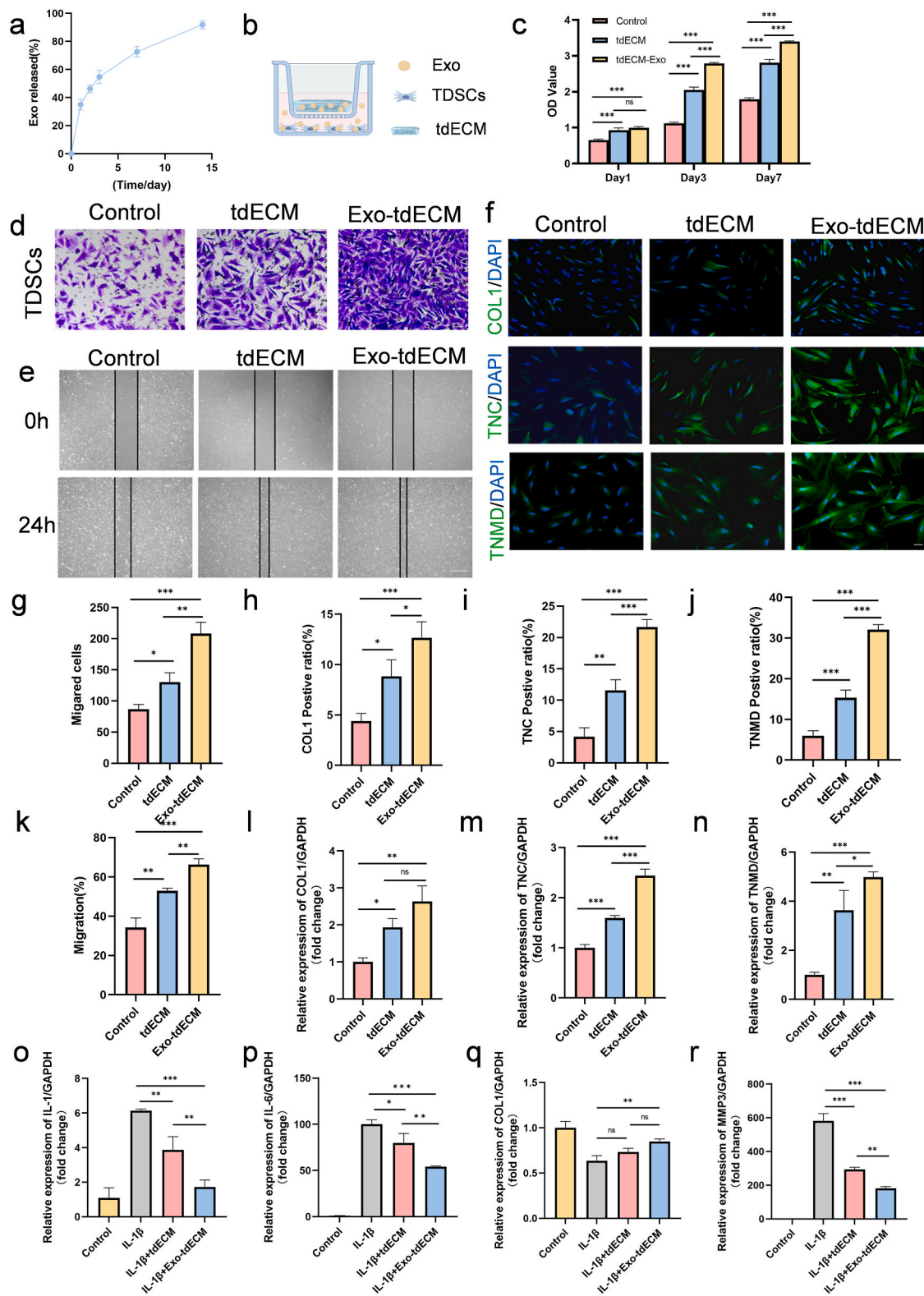


Fig. 5. Exo-tdECM promotes the proliferation, migration, and tenogenic differentiation of TDSCs, and inhibits TDSCs inflammation. (a) TDSCs-Exos release efficiency in tdECM hydrogel (n = 3). (b) In vitro co-culture was used to evaluate the effects of Exo-tdECM on the proliferation, migration, and tenogenic differentiation of TDSCs, and inhibit TDSC inflammation. (c) CCK-8 assay showing the TDSCs proliferation treated with tdECM and Exo-tdECM (n = 3/group). Scale bar = 50 μm. (d, g) Transwell assay showing the effect of tdECM and Exo-tdECM on the migration of TDSCs (n = 3/group). Scale bar = 500 μm. (e, k) Scratch assay showing the effect of tdECM and Exo-tdECM on the migration of TDSCs (n = 3/group). Scale bar = 500 μm. (f, h-j) Immunofluorescent staining of COL1, TNC, TNMD (green immunofluorescence) and DAPI (blue immunofluorescence) showing the effect of tdECM and Exo-tdECM on the tenogenic differentiation of TDSCs (n = 3/group). Scale bar = 50 μm. (l-n) RT-qPCR analysis of tenogenic differentiation genes relative mRNA level in TDSCs under different treatments (n = 3/group). (o-r) RT-qPCR analysis of pro-inflammatory genes relative mRNA level in TDSCs under different treatments (n = 3/group). *P < 0.05, **P < 0.01, ***P < 0.001, ns, nonsignificant difference.

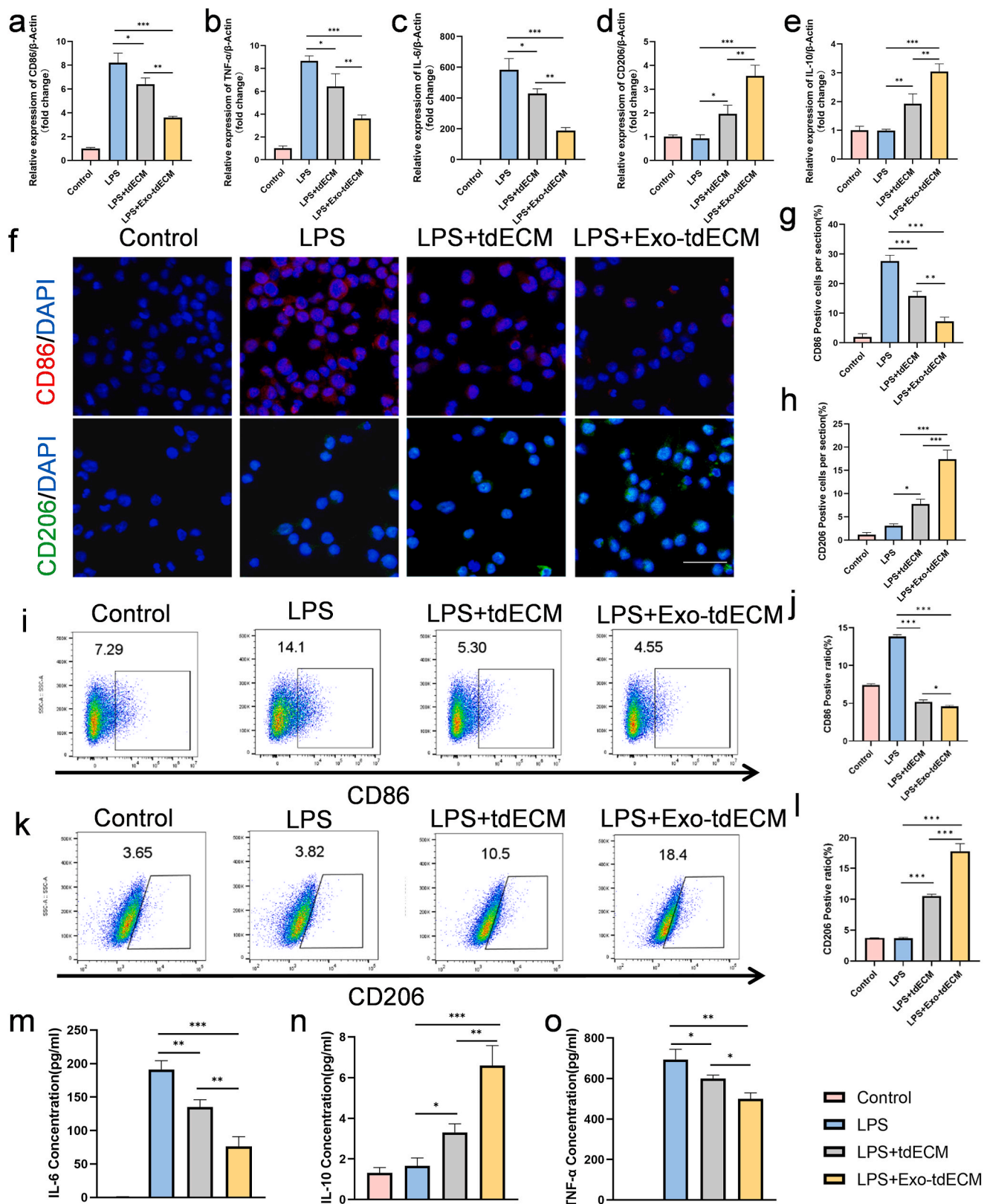


Fig. 6. Exo-tDECm promotes the polarization of macrophage M1 phenotype to M2 phenotype in vitro. (a–e) RT-qPCR analysis of macrophage polarization-related gene expression in THP-1 cells under different treatments (n = 3/group). (f–h) Immunofluorescent staining of iNOS, CD206 in THP-1 cells under different treatments (n = 3/group). Scale bar = 50 μ m. (i,j) Flow cytometry analysis of the M1 macrophage marker (CD86) in THP-1 cells under different treatments. (k,l) Flow cytometry analysis of the M2 macrophage marker (CD206) in THP-1 cells under different treatments (n = 3/group). (m–o) ELISA analysis of macrophage polarization-related cytokines (n = 3/group). *P < 0.05, **P < 0.01, ***P < 0.001, ns, nonsignificant difference.

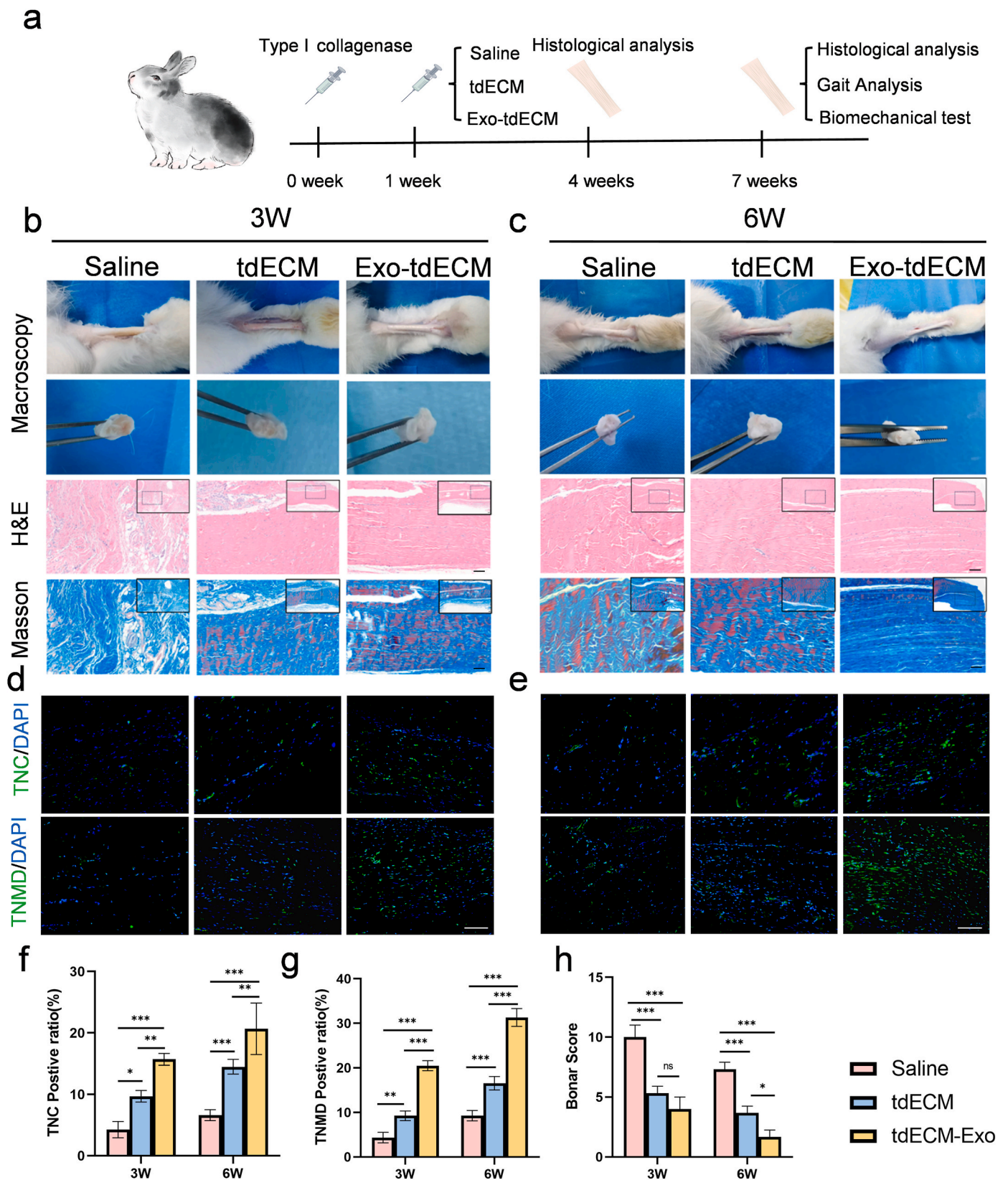


Fig. 7. Exo-ttECM enhances tendon regeneration in a rabbit Achilles tendinopathy model at macroscopic and histological levels. (a) A schematic illustration of the experimental animal design. (b,c) Representative histological images of Achilles tendons stained with macroscopic view, H&E staining and Masson staining from different groups at 3 weeks and 6 weeks. Scale bar = 100 μ m. (d–e) Representative Immunofluorescence staining images of TNC, TNMD of the tendon from different groups at 3 weeks and 6 weeks. Scale bar = 100 μ m. (f–g) Quantification of the TNC and TNMD positive ratio of the different groups' tendons (n = 3/group). (h) Bonar score used for semi-quantitative histology analysis of the different groups' tendons (n = 3/group). *P < 0.05, **P < 0.01, ***P < 0.001, ns, the nonsignificant difference.

elevated expression of tenogenic markers TNC and TNMD in tendons from the Exo-tdECM group, in comparison to those from the tdECM group and the saline group, at both 3 and 6 weeks (Fig. 7d–g). Upon conducting a semi-quantitative histological analysis using the Bonar score, which evaluates parameters such as cell morphology, cellularity, collagen derangement, and vascularity, it was observed that the Exo-tdECM group exhibited a significantly lower score compared to both the saline group and the tdECM group at the 6-week mark (Fig. 7h).

3.8. Exo-tdECM promotes M2 polarization and reduce M1 polarization of macrophages in vivo

To evaluate the influence of Exo-tdECM on macrophage polarization in vivo, immunofluorescent staining was employed to assess the extent of inflammatory infiltration across different experimental groups. At the 3-week mark, the Exo-tdECM group exhibited a significant reduction in the number of CD86-positive macrophages and a concomitant significant increase in the number of Arg1-positive macrophages, compared to the saline group (Fig. 8a,e,f). Simultaneously, there was a reduction in

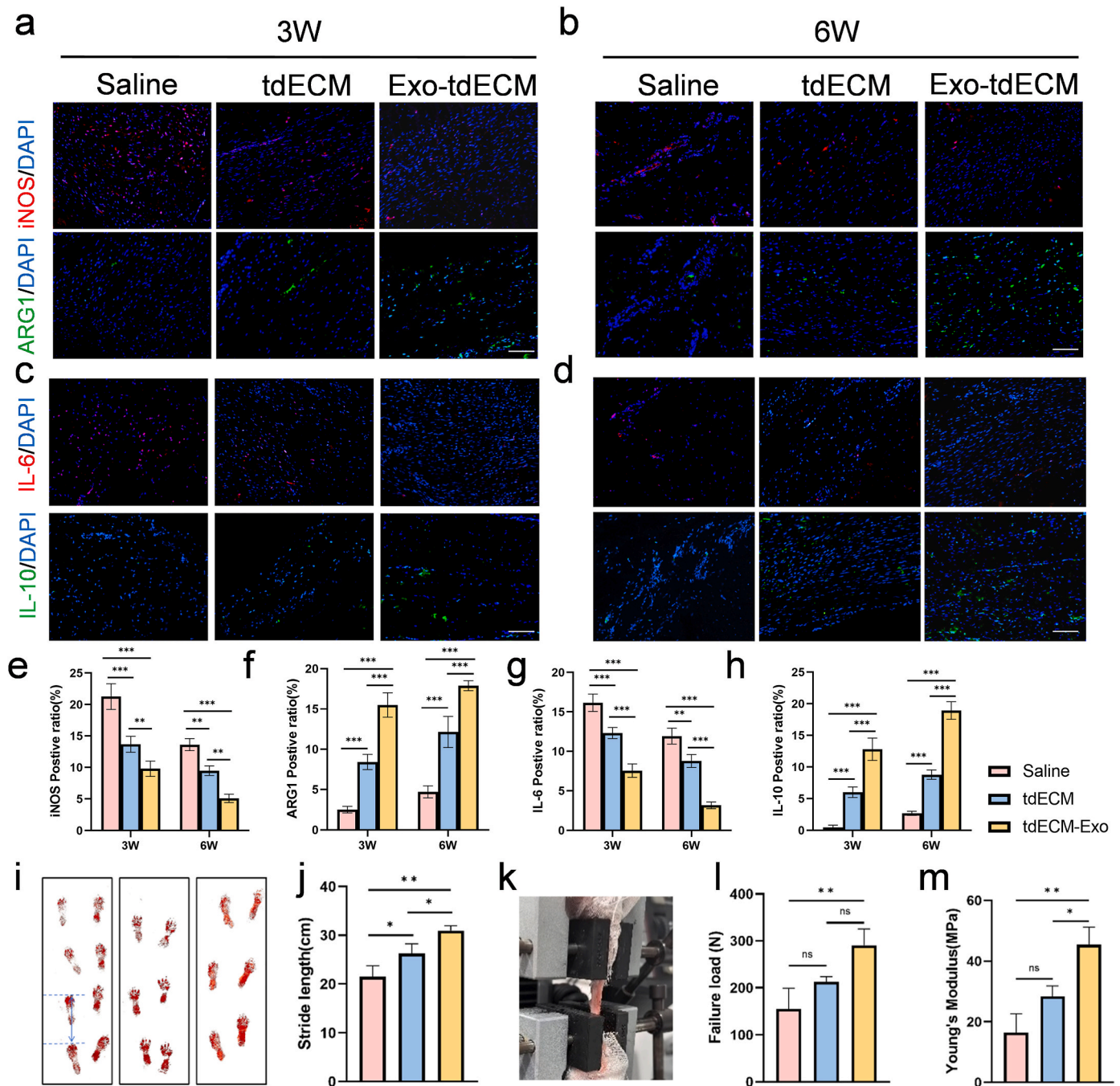


Fig. 8. Exos-ttECM regulates macrophage phenotype in a rabbit Achilles tendinopathy model. (a,b) Representative Immunofluorescence staining images of iNOS, ARG1 of the tendon from different groups at 3 weeks and 6 weeks. Scale bar = 100 μm. (c,d) Representative Immunofluorescence staining images of IL-6, IL-10 of tendon from different groups at 3 weeks and 6 weeks. Scale bar = 100 μm. (e–h) Quantification of iNOS, ARG1, IL-6, IL-10 positive ratio of tendons (n = 3/group) from different groups. (i) Representative images of gait analysis of rabbits with red ink on the back paws at 6 weeks. (j) Quantitative analysis of stride length from different groups (n = 3/group) at 6 weeks. (k) Biomechanical testing apparatus for tendons. (l–m) Failure load and Young's modulus of tendons (n = 3/group) from different groups at 6 w post-operation. *P < 0.05, **P < 0.01, ***P < 0.001, ns, nonsignificant difference.

the expression of the inflammatory marker IL-6, coupled with an increase in the expression of the anti-inflammatory marker IL-10 (Fig. 8c, g,h). The effect of tdECM treatment was intermediate. These findings imply that the combination of tdECM and exosomes can expedite the polarization of macrophages from the M1 phenotype to the M2 phenotype. At six weeks, a significant reduction in macrophage and inflammatory responses was observed across all groups (Fig. 8b,d,e-h). The Exo-tdECM group exhibited the most pronounced effect, followed by the tdECM group.

3.9. Exo-tdECM promotes tendinopathy-related gait and mechanical properties in vivo

The rabbits in the saline group exhibited the shortest average stride length of 21.51 ± 2.23 cm at 6 weeks. Compared with the saline group, the tdECM-Exo group's average stride length improved to 30.94 ± 0.99 cm, which was also notably better than the 26.26 ± 2.01 cm observed in the tdECM treated rabbits (Fig. 8i and j).

At 6 weeks, rabbit tendon samples were obtained and tested for mechanical stretch by a biomechanical tester (Fig. 8k). The failure load of the tdECM-Exo group was markedly greater than that of the saline group; however, no statistical difference was observed between the tdECM group and the Exo-tdECM group (Fig. 8l). No statistically significant difference in Young's modulus was seen between tendons treated with tdECM and those treated with saline; however, tendons treated with Exo-tdECM demonstrated a considerably greater Young's modulus than both the tdECM and saline groups (Fig. 8m). In summary, the Exo-tdECM group demonstrated superior mechanical qualities, succeeded by the tdECM group.

4. Discussion

Over the past few decades, numerous studies have demonstrated an inextricable link between inflammation and the onset and progression of tendinopathy [2,33]. During inflammatory states, the disruption of the normal homeostasis of the tendon physiological system frequently results in irreversible alterations in the structure and mechanics of the natural ECM [33]. Macrophages serve as crucial immune sentinels in tissue defense. They are often functionally categorized into two classes: M1 (classically activated) and M2 (alternatively activated) [37]. M2 macrophages are involved in regulating ECM balance and tissue healing, whereas M1 macrophages contribute to ECM degradation [38]. In this study, our findings demonstrated that (1) tdECM can facilitate the transformation of M1 macrophages into M2 macrophages during the early stages of tendon repair, and (2) tdECM hydrogel can serve as an effective carrier for exosomes. The functionality of injectable and sustainably released exosomes has been also demonstrated. And (3) The synergistic application of the tdECM hydrogel and TDSCs-Exos markedly enhanced anti-inflammatory effects and tendon repair in both in vitro and in vivo rabbit tendinopathy models. This research identifies the tdECM hydrogel as an innovative and efficient medium for the prolonged release of exosomes both in vitro and in vivo environments. Moreover, it is the first study to illustrate that the tdECM hydrogel promotes M2 macrophage polarization, thus producing an anti-inflammatory impact in vivo for the management of tendinopathy.

ECM serves as a crucial platform for cell attachment, communication, and interaction, thereby significantly influencing cell dynamics, behavior, and differentiation [39]. ECM predominantly consists of type I collagen, elastin, and proteoglycans, which collectively confer mechanical strength and elasticity to the tendon. Notably, collagen is of paramount importance, constituting the majority of the tendon's dry weight and playing a pivotal role in its structural integrity and functional capacity [40]. In recent years, biomimetic strategy-based engineered biomaterials, which possess the capability to reconstruct the ECM microenvironment, have demonstrated significant potential in the field of tissue engineering [41–43]. The administration of collagen

hydrogel serves to augment the collagen content within the tendon to a certain degree; however, the inherent pathological environment of the diseased tendon still poses significant challenges to its self-repair mechanisms. The development of ECM hydrogels introduces novel opportunities. Firstly, ECM hydrogels can directly replenish the extracellular matrix components that have been compromised by the lesion. Additionally, they have the capacity to modulate the microenvironment of the affected tendon. ECM hydrogels are capable of providing a microenvironment that is more physiologically relevant, facilitating long-term subculture and transplantation of organoids [44,45]. The degradation of the ECM results in the liberation of numerous bioactive constituents, including cryptic peptides, growth factors, and matrix metalloproteinases (MMPs), which play a significant role in endogenous cell recruitment and tissue remodeling [11,13,14,46]. The decellularized ECM hydrogel preserves various cell growth factors, such as transforming growth factors, which can promote cellular growth, migration, proliferation, differentiation, and angiogenesis [13]. Furthermore, tdECM hydrogel demonstrates enhanced cytocompatibility and a more porous architecture relative to traditional collagen hydrogels [12]. Additionally, dECM hydrogel facilitates the migration of stem cells and promotes the corresponding differentiation more effectively than traditional collagen hydrogels [12,47,48]. The tdECM hydrogel exhibits an elastic modulus of 4.35 ± 0.56 kPa. Although no studies have directly compared the mechanical properties of tdECM hydrogels with other materials, it is known that elastin and glycosaminoglycans (GAGs) are ECM components that enhance the mechanical properties and functionality of tendons. The Young's modulus of the bioprinted skeletal muscle dECM scaffold was markedly superior to that of the collagen I control [49]. The method of hydrogel application (printing/injection) and its degradation process also influence the mechanical properties of the hydrogel [15,50].

Numerous prior studies have investigated the use of decellularized ECM scaffolds embedded with stem cells or growth factors for the repair of tendon or ligament defects, demonstrating promising reparative outcomes [51–54]. Furthermore, research has been conducted on the development of tdECM membranes aimed at preventing tendon adhesion postoperatively [55]. Owing to their porous three-dimensional network structure and injectable properties, hydrogels can be directly administered to lesion sites in a minimally invasive manner, simultaneously facilitating cell delivery. This characteristic endows them with greater potential for application compared to traditional acellular scaffolds [13,56,57].

Nonetheless, current research on tdECM hydrogel remains predominantly focused on their role in promoting collagen synthesis [58]. The decellularized ECM primarily facilitates the recruitment of endogenous stem cells and immune cells to reconstruct the damaged microenvironment [59]. Research has demonstrated that proteins and GAGs within the ECM play a crucial role in the intrinsic regulation of cellular functions, including those of immune cells [60,61]. GAGs, as components of ECM, can guide macrophages toward a pro-healing mode [62]. Three-dimensional ECM networks can also promote M2 macrophages [62]. Softer dECM scaffolds were found to promote M2 polarization, indicating that substrate stiffness is a factor in inflammation [63]. A low pH value of 0.1 M hydrochloric acid can quicken the digestion of dECM powders, resulting in a softer dECM hydrogel, which shows improved stem cell proliferation and tendon-inducing ability compared to much stiffer dECM hydrogels [50]. This study utilized a 0.1M HCL concentration for digestion to synthesize a soft hydrogel aimed at enhancing stem cell proliferation and migration, promoting tendon differentiation, and improving anti-inflammatory properties for tendinopathy treatment. Furthermore, multiple studies have indicated that various natural materials, such as chitosan, can induce macrophage polarization [62,64,65]. ECM derived from porcine small intestinal submucosa has been demonstrated to facilitate the transition from the M1 macrophage phenotype to the M2 macrophage phenotype, which can effectively treat ulcerative colitis [18,59]. In this study, we observed that tdECM

hydrogel exhibits significant immunomodulatory effects on inflammatory TDCs and THP-1 macrophage cell lines in the context of tendinopathy, with these effects also being validated *in vivo*. Furthermore, a recent study has reported that tdECM can promote macrophage polarization, as evidenced by arginase and Griess assays [21].

As a small extracellular vesicle exhibiting biological properties akin to those of mesenchymal stem cells, exosomes hold significant promise in the field of regenerative medicine [28,66]. TDCs-Exos also represent a potential therapeutic strategy for tendon injuries [27,28]. Exosomes facilitate the healing of injured tendons not only by balancing the synthesis and degradation of the tendon extracellular matrix but also by modulating macrophage polarization [27]. The present investigation revealed that an elevation in TDCs-Exos concentration was associated with a gradual improvement in their ability to facilitate TDCs proliferation, migration, tendon differentiation, and anti-inflammatory responses. TDCs-Exos at a dose of 100 µg/mL demonstrated the most significant effects. However, there are currently two notable limitations: Firstly, the origin of exosomes is restricted, and their retention duration is brief. To facilitate its clinical application, a bioreactor may be employed to generate a substantial quantity of stem cells. Subsequently, exosome production can be enhanced through hypoxia treatment, regulation of the microenvironment's pH, and the application of cellular nanoporation technology. Moreover, the prolonged effects of exosomes can be achieved via carrier encapsulation. In recent years, attention has shifted towards the slow-release effect of exosomes encapsulated within hydrogels. This approach has been investigated for its potential in repairing skin, osteoarthritis, tendons, and other conditions [32,67,68]. This study has produced the tdECM hydrogel, which facilitates prolonged exosome release while mimicking the function of exosomes. This technique markedly reduces the number of exosomes required to attain similar reparative results. In comparison to conventional polymer materials and collagen hydrogels, tdECM hydrogel serves as a novel carrier that demonstrates enhanced biocompatibility and a greater abundance of growth factors and MMPs inherent to the native tendon microenvironment [11]. In this study, we introduce the application of tdECM hydrogel in the treatment of tendinopathy for the first time, highlighting its dual anti-inflammatory and pro-tendon repair effects as an injectable vehicle for exosomes. We conducted investigations of the release efficiency of TDCs-Exos both *in vitro* and *in vivo*, indicating that TDCs-Exos may remain within hydrogels for at least two weeks (Fig. 5a and S3). The retention time is markedly prolonged in comparison to the retention of isolated exosomes. This was the inaugural identification of its efficacy as a carrier for the sustained release of exosomes *in vitro* and *in vivo*. Second, while TDCs-Exos have been demonstrated to enhance tendon healing following injury, the precise mechanism by which TDCs-Exos influence macrophage polarization remains elusive. According to our KEGG environmental information processing analysis, the PI3K-Akt and MAPK signaling pathways emerged as the most enriched pathways (Fig. 4b). These pathways have been previously reported to play a critical role in regulating macrophage polarization and mitigating inflammation [69–72]. The predominant microRNA, miR-486-5p_R-1, constitutes 22 % of the total miRNA population and has been documented to significantly influence macrophage polarization via the PI3K-Akt signaling pathway [73]. Additionally, it has therapeutic potential for inflammation-related pulmonary diseases through the PI3K signaling pathway [74]. Future research will focus on elucidating the mechanisms by which miR-486-5p_R-1 exerts a more extensive role in tendon repair.

Based on the findings of this study, the tdECM hydrogel-based sustained-release exosome strategy emerges as a promising therapeutic approach. This method demonstrates dual efficacy in promoting macrophage polarization to the M2 phenotype, facilitating stem cell differentiation into tendon cells, enhancing type I collagen secretion, and supporting tendon regeneration. Concurrently, we identified specific miRNAs within the exosomes and conducted a comprehensive analysis of the components and pathways in exosomes that may be

implicated in these beneficial effects. Nevertheless, this study possesses certain limitations. Firstly, while we conducted miRNA sequencing on TDCs-Exos and undertook a preliminary investigation into the mechanism by which TDCs-Exos influences macrophage polarization and tendon repair, these findings have yet to be empirically validated. Secondly, the critical components and mechanisms by which tdECM hydrogel regulates macrophage polarization remain inadequately understood, representing a focal point for our future research endeavors. Prior research has elucidated the potential mechanisms through which ECM materials modulate macrophage polarization in the context of tissue regeneration. These mechanisms encompass the indirect regulation of growth factors and cytokines, alongside the binding of chemokines to inhibit the infiltration of inflammatory cells and restore a normal signaling milieu [60,75,76]. To optimize the anti-inflammatory properties of ECM materials and expand their application in therapeutic contexts, future research will focus on elucidating the key components and pathway mechanisms involved in the regulation of macrophages by ECM materials. Finally, tendon repair and regeneration is a protracted process comprising several physiological phases: inflammation, proliferation, remodeling, and maturity. The follow-up of this study concluded 6 weeks post-treatment and the tendon was not fully repaired at that time; thus, the effects in the latter stages require more investigation to assess both the long-term regenerative outcomes and the functionality of the regenerated tendon.

5. Conclusion

This study represents the first investigation into the effect of tdECM hydrogel on promoting M2 polarization of macrophages *in vivo* in tendinopathy. By employing tdECM hydrogel as a carrier for the sustained release of TDCs-Exos, we achieved a dual effect by improving the microenvironment: enhancing M2 macrophage polarization and promoting tendon differentiation of stem cells along with type I collagen synthesis, thereby facilitating the repair of tendinopathy. These findings elucidate the unique role of tdECM hydrogel in immune regulation and underscore a novel and effective therapeutic strategy for the treatment of tendinopathy and other inflammatory diseases.

CRedit authorship contribution statement

Danmei Li: Writing – original draft, Methodology, Investigation, Formal analysis, Data curation, Conceptualization. **Shuai Li:** Writing – review & editing, Investigation, Conceptualization. **Shukun He:** Writing – review & editing, Methodology, Data curation. **Hongpu He:** Methodology, Investigation. **Guangxun Yuan:** Data curation. **Binbin Ma:** Validation, Investigation. **Yijun Zhang:** Investigation, Conceptualization. **Chengjie Yuan:** Investigation, Conceptualization. **Zhiqin Liu:** Methodology. **Zhenhan Deng:** Writing – review & editing, Conceptualization. **Jian Xu:** Writing – review & editing, Supervision, Funding acquisition, Conceptualization.

Ethics approval and consent to participate

All animal experimental procedures received approval from the Laboratory Animal Welfare and Ethics Review Committee of Zhejiang University (Approval Number: ZJU20240230) and the Tab of Animal Experimental Ethical Inspection of the First Affiliated Hospital, Zhejiang University School of Medicine (Approval Number: 20,241,705).

Declaration of competing interest

The authors declare no conflict of interest.

Acknowledgments

This study was supported by the National Natural Science

Foundation of China (82102632,82160412), Zhejiang Provincial Natural Science Foundation of China under Grant No. LMS25H060003 and No. LQ23H060005, Zhejiang Province Medical and Health Scientific Research Project (No. 2025KY054), Zhejiang Traditional Chinese Medicine Administration Bureau (Project: No. 2025ZL382) and the Guangdong Basic and Applied Basic Research Foundation (2023A1515220072).

Appendix A. Supplementary data

Supplementary data to this article can be found online at <https://doi.org/10.1016/j.bioactmat.2025.01.016>.

References

- [1] S.P. Magnusson, H. Langberg, M. Kjaer, The pathogenesis of tendinopathy: balancing the response to loading, *Nat. Rev. Rheumatol.* 6 (5) (2010) 262–268, <https://doi.org/10.1038/nrrheum.2010.43>.
- [2] N.L. Millar, K.G. Silbernagel, K. Thorborg, P.D. Kirwan, L.M. Galatz, G.D. Abrams, G. Murrell, I.B. McInnes, S.A. Rodeo, Tendinopathy, *Nat. Rev. Dis. Primers* 7 (1) (2021) 1, <https://doi.org/10.1038/s41572-020-00234-1>.
- [3] U.M. Kujala, S. Sarna, J. Kaprio, Cumulative incidence of achilles tendon rupture and tendinopathy in male former elite athletes, *Clin. J. Sport Med.* 15 (3) (2005) 133–135, <https://doi.org/10.1097/01.jsm.0000165347.55638.23>.
- [4] N. Kakouris, N. Yener, D. Fong, A. Cumulative incidence of running-related musculoskeletal injuries in runners, *J. Sport Health Sci.* 10 (5) (2021) 513–522, <https://doi.org/10.1016/j.jshs.2021.04.001>.
- [5] M. Abate, K.G. Silbernagel, C. Siljeholm, A. Di Iorio, D. De Amicis, V. Salini, S. Werner, R. Paganelli, Pathogenesis of tendinopathies: inflammation or degeneration? *Arthritis Res. Ther.* 11 (3) (2009) 235, <https://doi.org/10.1186/ar2723>.
- [6] S.G. Dakin, J. Dudhia, R.K. Smith, Resolving an inflammatory concept: the importance of inflammation and resolution in tendinopathy, *Vet. Immunol. Immunopathol.* 158 (3–4) (2014) 121–127, <https://doi.org/10.1016/j.vetimm.2014.01.007>.
- [7] P. Sharma, M. Maffulli, Tendon injury and tendinopathy: healing and repair, *J. Bone. Joint. Surg. Am.* 87 (1) (2005) 187–202, <https://doi.org/10.2106/JBJS.D.01850>.
- [8] J.Y. Sunwoo, C.D. Eliasberg, C.B. Carballo, S.A. Rodeo, The role of the macrophage in tendinopathy and tendon healing, *J. Orthop. Res.* 38 (8) (2020) 1666–1675, <https://doi.org/10.1002/jor.24667>.
- [9] K. Knobloch, Eccentric rehabilitation exercise increases peritendinous type I collagen synthesis in humans with achilles tendinosis, *Scand. J. Med. Sci. Sports* 17 (3) (2007) 298–299, <https://doi.org/10.1111/j.1600-0838.2007.00652.x>.
- [10] S.S. Raghavan, C.Y. Woon, A. Kraus, K. Megerle, M.S. Choi, B.C. Pridgen, H. Pham, J. Chang, Human flexor tendon tissue engineering: decellularization of human flexor tendons reduces immunogenicity in vivo, *Tissue Eng. Part A* 18 (7–8) (2012) 796–805, <https://doi.org/10.1089/ten.TEA.2011.0422>.
- [11] S. Anjum, T. Li, M. Saeed, Q. Ao, Exploring polysaccharide and protein-enriched decellularized matrix scaffolds for tendon and ligament repair: a review, *Int. J. Biol. Macromol.* 254 (Pt 2) (2024) 127891, <https://doi.org/10.1016/j.ijbiomac.2023.127891>.
- [12] L.J. Ning, Y.J. Zhang, Y.J. Zhang, M. Zhu, W. Ding, Y.L. Jiang, Y. Zhang, J.C. Luo, T.W. Qin, Enhancement of migration and tenogenic differentiation of macaca mulatta tendon-derived stem cells by decellularized tendon hydrogel, *Front. Cell Dev. Biol.* 9 (2021) 651583, <https://doi.org/10.3389/fcell.2021.651583>.
- [13] W. Zhang, A. Du, S. Liu, M. Lv, S. Chen, Research progress in decellularized extracellular matrix-derived hydrogels, *Regen. Ther.* 18 (2021) 88–96, <https://doi.org/10.1016/j.reth.2021.04.002>.
- [14] V. Agrawal, J. Kelly, S. Tottey, K.A. Daly, S.A. Johnson, B.F. Siu, J. Reing, S. F. Badyal, An isolated cryptic peptide influences osteogenesis and bone remodeling in an adult mammalian model of digit amputation, *Tissue Eng. Part A* 17 (23–24) (2011) 3033–3044, <https://doi.org/10.1089/ten.TEA.2011.0257>.
- [15] M. Brown, J. Li, C. Moraes, M. Tabrizian, N. Li-Jessen, Decellularized extracellular matrix: new promising and challenging biomaterials for regenerative medicine, *Biomaterials* 289 (2022) 121786, <https://doi.org/10.1016/j.biomaterials.2022.121786>.
- [16] W. Liu, X. Zhang, X. Jiang, B. Dai, L. Zhang, Y. Zhu, Decellularized extracellular matrix materials for treatment of ischemic cardiomyopathy, *Bioact. Mater.* 33 (2024) 460–482, <https://doi.org/10.1016/j.bioactmat.2023.10.015>.
- [17] A. Franklin, M.J. Gi, H. Oda, Y. Kaizawa, J. Leyden, Z. Wang, J. Chang, P.M. Fox, Homing of adipose-derived stem cells to a tendon-derived hydrogel: a potential mechanism for improved tendon-bone interface and tendon healing, *J. Hand. Surg. Am.* 45 (12) (2020) 1180–1181, <https://doi.org/10.1016/j.jhss.2020.05.003>.
- [18] T.J. Keane, J. Dziki, E. Sobieski, A. Smoulder, A. Castleton, N. Turner, L.J. White, S. F. Badyal, Restoring mucosal barrier function and modifying macrophage phenotype with an extracellular matrix hydrogel: potential therapy for ulcerative colitis, *J. Crohns Colitis* 11 (3) (2017) 360–368, <https://doi.org/10.1093/ecco-jcc/jjw149>.
- [19] M. Becker, J.A. Maring, M. Schneider, M.A. Herrera, M. Seifert, O. Klein, T. Braun, V. Falk, C. Stamm, Towards a novel patch material for cardiac applications: tissue-specific extracellular matrix introduces essential key features to decellularized amniotic membrane, *Int. J. Mol. Sci.* 19 (4) (2018), <https://doi.org/10.3390/ijms19041032>.
- [20] M. Deng, J. Tan, C. Hu, T. Hou, W. Peng, J. Liu, B. Yu, Q. Dai, J. Zhou, Y. Yang, R. Dong, C. Ruan, S. Dong, J. Xu, Modification of plga scaffold by msc-derived extracellular matrix combats macrophage inflammation to initiate bone regeneration via tgf-beta-induced protein, *Adv. Health. Mater.* 9 (13) (2020) e2000353, <https://doi.org/10.1002/adhm.202000353>.
- [21] A. Bhatt, N. Dhiman, P.S. Giri, G.N. Kasinathan, F. Pati, S.N. Rath, Biocompatibility-on-a-chip: characterization and evaluation of decellularized tendon extracellular matrix (tdecM) hydrogel for 3d stem cell culture in a microfluidic device, *Int. J. Biol. Macromol.* 213 (2022) 768–779, <https://doi.org/10.1016/j.ijbiomac.2022.06.010>.
- [22] H. Shao, H. Im, C.M. Castro, X. Breakefield, R. Weissleder, H. Lee, New technologies for analysis of extracellular vesicles, *Chem. Rev.* 118 (4) (2018) 1917–1950, <https://doi.org/10.1021/acs.chemrev.7b00534>.
- [23] S. Keshkar, N. Azarpira, M.H. Ghahremani, Mesenchymal stem cell-derived extracellular vesicles: novel frontiers in regenerative medicine, *Stem Cell Res. Ther.* 9 (1) (2018) 63, <https://doi.org/10.1186/s13287-018-0791-7>.
- [24] H. Valadi, K. Ekstrom, A. Bossios, M. Sjostrand, J.J. Lee, J.O. Lotvall, Exosome-mediated transfer of mRNAs and microRNAs is a novel mechanism of genetic exchange between cells, *Nat. Cell Biol.* 9 (6) (2007) 654–659, <https://doi.org/10.1038/ncb1596>.
- [25] X. Zhang, W. Song, Y. Liu, K. Han, Y. Wu, E. Cho, Z. Fang, L. Jiang, Y. Hu, X. Zhu, J. Jiang, X. Huangfu, J. Zhao, Healthy tendon stem cell-derived exosomes promote tendon-to-bone healing of aged chronic rotator cuff tears by breaking the positive-feedback cross-talk between senescent tendon stem cells and macrophages through the modulation of macrophage polarization, *Small* 20 (31) (2024) e2311033, <https://doi.org/10.1002/sml.202311033>.
- [26] C. Wang, Y. Zhang, G. Zhang, W. Yu, Y. He, Adipose stem cell-derived exosomes ameliorate chronic rotator cuff tendinopathy by regulating macrophage polarization: from a mouse model to a study in human tissue, *Am. J. Sports Med.* 49 (9) (2021) 2321–2331, <https://doi.org/10.1177/03635465211020010>.
- [27] T. Ye, Z. Chen, J. Zhang, L. Luo, R. Gao, L. Gong, Y. Du, Z. Xie, B. Zhao, Q. Li, Y. Wang, Large extracellular vesicles secreted by human ipsc-derived mscs ameliorate tendinopathy via regulating macrophage heterogeneity, *Bioact. Mater.* 21 (2023) 194–208, <https://doi.org/10.1016/j.bioactmat.2022.08.007>.
- [28] Y. Wang, G. He, Y. Guo, H. Tang, Y. Shi, X. Bian, M. Zhu, X. Kang, M. Zhou, J. Lyu, M. Yang, M. Mu, F. Lai, K. Lu, W. Chen, B. Zhou, J. Zhang, K. Tang, Exosomes from tendon stem cells promote injury tendon healing through balancing synthesis and degradation of the tendon extracellular matrix, *J. Cell Mol. Med.* 23 (8) (2019) 5475–5485, <https://doi.org/10.1111/jcmm.14430>.
- [29] G. Jiang, Y. Wu, J. Meng, F. Wu, S. Li, M. Lin, X. Gao, J. Hong, W. Chen, S. Yan, R. Yan, G. Feng, Z. Cheng, Comparison of leukocyte-rich platelet-rich plasma and leukocyte-poor platelet-rich plasma on achilles tendinopathy at an early stage in a rabbit model, *Am. J. Sports Med.* 48 (5) (2020) 1189–1199, <https://doi.org/10.1177/0363546520906142>.
- [30] D. Ruan, Y. Fei, S. Qian, Z. Huang, W. Chen, C. Tang, X. Xiang, J. Xu, Z. Yin, X. Chen, B.C. Heng, W. Liu, W. Shen, H. Ouyang, Early-stage primary anti-inflammatory therapy enhances the regenerative efficacy of platelet-rich plasma in a rabbit achilles tendinopathy model, *Am. J. Sports Med.* 49 (12) (2021) 3357–3371, <https://doi.org/10.1177/03635465211037354>.
- [31] N. Maffulli, U.G. Longo, F. Franceschi, C. Rabbitt, V. Denaro, Movin and bonar scores assess the same characteristics of tendon histology, *Clin. Orthop. Relat. Res.* 466 (7) (2008) 1605–1611, <https://doi.org/10.1007/s11999-008-0261-0>.
- [32] H. Yu, J. Cheng, W. Shi, B. Ren, F. Zhao, Y. Shi, P. Yang, X. Duan, J. Zhang, X. Fu, X. Hu, Y. Ao, Bone marrow mesenchymal stem cell-derived exosomes promote tendon regeneration by facilitating the proliferation and migration of endogenous tendon stem/progenitor cells, *Acta Biomater.* 106 (2020) 328–341, <https://doi.org/10.1016/j.actbio.2020.01.051>.
- [33] M. Zhang, H. Liu, Q. Cui, P. Han, S. Yang, M. Shi, T. Zhang, Z. Zhang, Z. Li, Tendon stem cell-derived exosomes regulate inflammation and promote the high-quality healing of injured tendon, *Stem Cell Res. Ther.* 11 (1) (2020) 402, <https://doi.org/10.1186/s13287-020-01918-x>.
- [34] K. Zhang, Y. Yang, H. Ge, J. Wang, X. Chen, X. Lei, J. Zhong, C. Zhang, J. Xian, Y. Lu, L. Tan, H. Feng, Artesunate promotes the proliferation of neural stem/progenitor cells and alleviates ischemia-reperfusion injury through pi3k/akt/foxo-3a/p27(kip1) signaling pathway, *Aging (Albany Ny)* 12 (9) (2020) 8029–8048, <https://doi.org/10.18632/aging.103121>.
- [35] J. Qu, J. Li, Y. Zhang, R. He, X. Liu, K. Gong, L. Duan, W. Luo, Z. Hu, G. Wang, C. Xia, D. Luo, Akr1b10 promotes breast cancer cell proliferation and migration via the pi3k/akt/nf-kappab signaling pathway, *Cell Biosci.* 11 (1) (2021) 163, <https://doi.org/10.1186/s13578-021-00677-3>.
- [36] D. Wei, B. Rui, F. Qingquan, C. Chen, H.Y. Ping, S. Xiaoling, W. Hao, G. Jun, Kif11 promotes cell proliferation via erbB2/pi3k/akt signaling pathway in gallbladder cancer, *Int. J. Biol. Sci.* 17 (2) (2021) 514–526, <https://doi.org/10.7150/ijbs.54074>.
- [37] A. Sica, A. Mantovani, Macrophage plasticity and polarization: in vivo veritas, *J. Clin. Invest.* 122 (3) (2012) 787–795, <https://doi.org/10.1172/JCI59643>.
- [38] N.L. Millar, G.A. Murrell, I.B. McInnes, Inflammatory mechanisms in tendinopathy - towards translation, *Nat. Rev. Rheumatol.* 13 (2) (2017) 110–122, <https://doi.org/10.1038/nrrheum.2016.213>.
- [39] M. Hu, Z. Ling, X. Ren, Extracellular matrix dynamics: tracking in biological systems and their implications, *J. Biol. Eng.* 16 (1) (2022) 13, <https://doi.org/10.1186/s13036-022-00292-x>.

- [40] Y. Liu, C.W. Suen, J.F. Zhang, G. Li, Current concepts on tenogenic differentiation and clinical applications, *J. Orthop. Trans.* 9 (2017) 28–42, <https://doi.org/10.1016/j.jot.2017.02.005>.
- [41] Z. Zhao, X. Xia, J. Liu, M. Hou, Y. Liu, Z. Zhou, Y. Xu, F. He, H. Yang, Y. Zhang, C. Ruan, X. Zhu, Cartilage-inspired self-assembly glycopeptide hydrogels for cartilage regeneration via ROS scavenging, *Bioact. Mater.* 32 (2024) 319–332, <https://doi.org/10.1016/j.bioactmat.2023.10.013>.
- [42] X. Zhai, C. Ruan, Y. Ma, D. Cheng, M. Wu, W. Liu, X. Zhao, H. Pan, W.W. Lu, 3D-bioprinted osteoblast-laden nanocomposite hydrogel constructs with induced microenvironments promote cell viability, differentiation, and osteogenesis both in vitro and in vivo, *Adv. Sci.* 5 (3) (2018) 1700550, <https://doi.org/10.1002/adv.201700550>.
- [43] B.S. Kim, S. Das, J. Jang, D.W. Cho, Decellularized extracellular matrix-based bioinks for engineering tissue- and organ-specific microenvironments, *Chem. Rev.* 120 (19) (2020) 10608–10661, <https://doi.org/10.1021/acs.chemrev.9b00808>.
- [44] C. Li, N. An, Q. Song, Y. Hu, W. Yin, Q. Wang, Y. Le, W. Pan, X. Yan, Y. Wang, J. Liu, Enhancing organoid culture: harnessing the potential of decellularized extracellular matrix hydrogels for mimicking microenvironments, *J. Biomed. Sci.* 31 (1) (2024) 96, <https://doi.org/10.1186/s12929-024-01086-7>.
- [45] S. Kim, S. Min, Y.S. Choi, S.H. Jo, J.H. Jung, K. Han, J. Kim, S. An, Y.W. Ji, Y. G. Kim, S.W. Cho, Tissue extracellular matrix hydrogels as alternatives to matrigel for culturing gastrointestinal organoids, *Nat. Commun.* 13 (1) (2022) 1692, <https://doi.org/10.1038/s41467-022-29279-4>.
- [46] J.K. Kular, S. Basu, R.I. Sharma, The extracellular matrix: structure, composition, age-related differences, tools for analysis and applications for tissue engineering, *J. Tissue Eng.* 5 (2014) 1548680776, <https://doi.org/10.1177/2041731414557112>.
- [47] S. Chae, S.S. Lee, Y.J. Choi, D.H. Hong, G. Gao, J.H. Wang, D.W. Cho, 3D cell-printing of biocompatible and functional meniscus constructs using meniscus-derived bioink, *Biomaterials* 267 (2021) 120466, <https://doi.org/10.1016/j.biomaterials.2020.120466>.
- [48] N. Rao, G. Agmon, M.T. Tierney, J.L. Ungerleider, R.L. Braden, A. Sacco, K. L. Christman, Engineering an injectable muscle-specific microenvironment for improved cell delivery using a nanofibrous extracellular matrix hydrogel, *ACS Nano* 11 (4) (2017) 3851–3859, <https://doi.org/10.1021/acs.nano.7b00093>.
- [49] Y.J. Choi, T.G. Kim, J. Jeong, H.G. Yi, J.W. Park, W. Hwang, D.W. Cho, 3D cell printing of functional skeletal muscle constructs using skeletal muscle-derived bioink, *Adv. Health. Mater.* 5 (20) (2016) 2636–2645, <https://doi.org/10.1002/adhm.201600483>.
- [50] F. Zhao, J. Cheng, J. Zhang, H. Yu, W. Dai, W. Yan, M. Sun, G. Ding, Q. Li, Q. Meng, Q. Liu, X. Duan, X. Hu, Y. Ao, Comparison of three different acidic solutions in tendon decellularized extracellular matrix bio-ink fabrication for 3D cell printing, *Acta Biomater.* 131 (2021) 262–275, <https://doi.org/10.1016/j.actbio.2021.06.026>.
- [51] C.S. Chamberlain, A. Clements, J.A. Kink, U. Choi, G.S. Baer, M.A. Halanski, P. Hematti, R. Vanderby, Extracellular vesicle-educated macrophages promote early achilles tendon healing, *Stem. Cells* 37 (5) (2019) 652–662, <https://doi.org/10.1002/stem.2988>.
- [52] N. K. V. Ca, J. Joseph, A. U. A. John, A. Abraham, Mesenchymal stem cells seeded decellularized tendon scaffold for tissue engineering, *Curr. Stem Cell Res. Ther.* 16 (2) (2021) 155–164, <https://doi.org/10.2174/1574888X15666200723123901>.
- [53] M. Bottagisio, D. D'Arrigo, G. Talo, M. Bongio, M. Ferroni, F. Boschetti, M. Moretti, A.B. Lovati, Achilles tendon repair by decellularized and engineered xenografts in a rabbit model, *Stem Cells Int.* 2019 (2019) 5267479, <https://doi.org/10.1155/2019/5267479>.
- [54] H. Xiao, Y. Chen, M. Li, Q. Shi, Y. Xu, J. Hu, X. Li, C. Chen, H. Lu, Cell-free book-shaped decellularized tendon matrix graft capable of controlled release of bmp-12 to improve tendon healing in a rat model, *Am. J. Sports Med.* 49 (5) (2021) 1333–1347, <https://doi.org/10.1177/0363546521994555>.
- [55] S. Yao, Z. Liang, Y.W. Lee, P. Yung, P. Lui, Bioactive decellularized tendon-derived stem cell sheet for promoting graft healing after anterior cruciate ligament reconstruction, *Am. J. Sports Med.* 51 (1) (2023) 66–80, <https://doi.org/10.1177/03635465221135770>.
- [56] S. Almawash, S.K. Osman, G. Mustafa, H.M. El, Current and future prospective of injectable hydrogels-design challenges and limitations, *Pharmaceuticals* 15 (3) (2022), <https://doi.org/10.3390/ph15030371>.
- [57] L.T. Saldin, M.C. Cramer, S.S. Velankar, L.J. White, S.F. Badylak, Extracellular matrix hydrogels from decellularized tissues: structure and function, *Acta Biomater.* 49 (2017) 1–15, <https://doi.org/10.1016/j.actbio.2016.11.068>.
- [58] Z. Chen, Y. Rui, Y. Xu, Q. Zhang, Z. Sun, J. Zhou, X. Chen, Effect of tendon hydrogel on healing of tendon injury, *Exp. Ther. Med.* 14 (5) (2017) 3955–3960, <https://doi.org/10.3892/etm.2017.5020>.
- [59] M. Tao, F. Liang, J. He, W. Ye, R. Javed, W. Wang, T. Yu, J. Fan, X. Tian, X. Wang, W. Hou, Q. Ao, Decellularized tendon matrix membranes prevent post-surgical tendon adhesion and promote functional repair, *Acta Biomater.* 134 (2021) 160–176, <https://doi.org/10.1016/j.actbio.2021.07.038>.
- [60] B.M. Sicari, J.L. Dziki, B.F. Siu, C.J. Medberry, C.L. Dearth, S.F. Badylak, The promotion of a constructive macrophage phenotype by solubilized extracellular matrix, *Biomaterials* 35 (30) (2014) 8605–8612, <https://doi.org/10.1016/j.biomaterials.2014.06.060>.
- [61] M. Friedemann, L. Kalbitzer, S. Franz, S. Moeller, M. Schnabelrauch, J.C. Simon, T. Pompe, K. Franke, Instructing human macrophage polarization by stiffness and glycosaminoglycan functionalization in 3D collagen networks, *Adv. Health. Mater.* 6 (7) (2017), <https://doi.org/10.1002/adhm.201600967>.
- [62] M. Torregrossa, A. Kakpenova, J.C. Simon, S. Franz, Modulation of macrophage functions by ecm-inspired wound dressings - a promising therapeutic approach for chronic wounds, *Biol. Chem.* 402 (11) (2021) 1289–1307, <https://doi.org/10.1515/hsz-2021-0145>.
- [63] R.X. Wu, X.T. He, J.H. Zhu, Y. Yin, X. Li, X. Liu, F.M. Chen, Modulating macrophage responses to promote tissue regeneration by changing the formulation of bone extracellular matrix from filler particles to gel bioscaffolds, *Mater. Sci. Eng. C-Mater. Biol. Appl.* 101 (2019) 330–340, <https://doi.org/10.1016/j.msec.2019.03.107>.
- [64] D.P. Vasconcelos, A.C. Fonseca, M. Costa, I.F. Amaral, M.A. Barbosa, A.P. Aguiar, J. N. Barbosa, Macrophage polarization following chitosan implantation, *Biomaterials* 34 (38) (2013) 9952–9959, <https://doi.org/10.1016/j.biomaterials.2013.09.012>.
- [65] S.H. Chang, Y.Y. Lin, G.J. Wu, C.H. Huang, G.J. Tsai, Effect of chitosan molecular weight on anti-inflammatory activity in the raw 264.7 macrophage model, *Int. J. Biol. Macromol.* 131 (2019) 167–175, <https://doi.org/10.1016/j.ijbiomac.2019.02.066>.
- [66] H. Ruan, Y. Li, D. Zheng, L. Deng, G. Chen, X. Zhang, Y. Tang, W. Cui, Engineered extracellular vesicles for ischemic stroke treatment, *Innovation (Camb)* 4 (2) (2023) 100394, <https://doi.org/10.1016/j.xinn.2023.100394>.
- [67] Y. Zhang, X. Wang, J. Chen, D. Qian, P. Gao, T. Qin, T. Jiang, J. Yi, T. Xu, Y. Huang, Q. Wang, Z. Zhou, T. Bao, X. Zhao, H. Liu, Z. Zheng, J. Fan, S. Zhao, Q. Li, G. Yin, Exosomes derived from platelet-rich plasma administration in site mediate cartilage protection in subtalar osteoarthritis, *J. Nanobiotechnology* 20 (1) (2022) 56, <https://doi.org/10.1186/s12951-022-01245-8>.
- [68] S.C. Tao, S.C. Guo, M. Li, Q.F. Ke, Y.P. Guo, C.Q. Zhang, Chitosan wound dressings incorporating exosomes derived from microRNA-126-overexpressing synovium mesenchymal stem cells provide sustained release of exosomes and heal full-thickness skin defects in a diabetic rat model, *Stem Cells Trans. Med.* 6 (3) (2017) 736–747, <https://doi.org/10.5966/scm.2016-0275>.
- [69] L. Li, W. Jiang, B. Yu, H. Liang, S. Mao, X. Hu, Y. Feng, J. Xu, L. Chu, Quercetin improves cerebral ischemia/reperfusion injury by promoting microglia/macrophages m2 polarization via regulating pi3k/akt/nf-kappab signaling pathway, *Biomed. Pharmacother.* 168 (2023) 115653, <https://doi.org/10.1016/j.biopha.2023.115653>.
- [70] X. Liu, Y. Wang, P. Shao, Y. Chen, C. Yang, J. Wang, S. Cui, Sargentodoxa cuneata and patrinia villosa extract inhibits lps-induced inflammation by shifting macrophages polarization through fak/pi3k/akt pathway regulation and glucose metabolism reprogramming, *J. Ethnopharmacol.* 318 (Pt A) (2024) 116855, <https://doi.org/10.1016/j.jep.2023.116855>.
- [71] T. Liu, M. Xu, Z. Shi, M. Li, R. Wang, Y. Shi, X. Xu, T. Shao, Q. Sun, Shenhua plaster ameliorates the inflammation of postoperative ileus through inhibiting pi3k/akt/nf-kappab pathway, *Biomed. Pharmacother.* 156 (2022) 113922, <https://doi.org/10.1016/j.biopha.2022.113922>.
- [72] J. Yan, G. Feng, Y. Yang, X. Zhao, L. Ma, H. Guo, X. Chen, H. Wang, Z. Chen, Q. Jin, Nintedanib ameliorates osteoarthritis in mice by inhibiting synovial inflammation and fibrosis caused by m1 polarization of synovial macrophages via the mapk/pi3k-akt pathway, *Faseb. J.* 37 (10) (2023) e23177, <https://doi.org/10.1096/fj.202300944RR>.
- [73] W. Su, Y. Yin, J. Zhao, R. Hu, H. Zhang, J. Hu, R. Ren, Y. Zhang, A. Wang, Z. Lyu, Y. Mu, Y. Cheng, Exosomes derived from umbilical cord-derived mesenchymal stem cells exposed to diabetic microenvironment enhance m2 macrophage polarization and protect against diabetic nephropathy, *Faseb. J.* 38 (14) (2024) e23798, <https://doi.org/10.1096/fj.202400359R>.
- [74] D. Tian, Y. Miao, W. Hao, N. Yang, P. Wang, Q. Ge, C. Zhang, Tanshinone iia protects against chronic obstructive pulmonary disease via exosome-shuttled mir-486-5p, *Int. J. Mol. Med.* 50 (1) (2022), <https://doi.org/10.3892/ijmm.2022.5153>.
- [75] M.C. Cramer, S.F. Badylak, Extracellular matrix-based biomaterials and their influence upon cell behavior, *Ann. Biomed. Eng.* 48 (7) (2020) 2132–2153, <https://doi.org/10.1007/s10439-019-02408-9>.
- [76] U. Freudenberg, Y. Liang, K.L. Kiick, C. Werner, Glycosaminoglycan-based biohybrid hydrogels: a sweet and smart choice for multifunctional biomaterials, *Adv. Mater.* 28 (40) (2016) 8861–8891, <https://doi.org/10.1002/adma.201601908>.